universität wien

MASTERARBEIT / MASTER'S THESIS

Titel der Masterarbeit / Title of the Master's Thesis

„The potential of Drone-base Geology:
An innovative way of gathering geological data."

verfasst von / submitted by

Maximilian-Zak Schaschl, BSc

angestrebter akademischer Grad / in partial fulfilment of the requirements for the degree of

Master of Science(MSc)
Master of Science(MSc)

Wien, 2018 / Vienna 2018

Studienkennzahl lt. Studienblatt / degree programme code as it appears on the student record sheet:	A 066 815
Studienrichtung lt. Studienblatt / degree programme as it appears on the student record sheet:	Erdwissenschaften / Earthsciences
Betreut von / Supervisor:	Univ.-Prof. Mag. Dr. Bernhard Grasemann

Eidesstattliche Erklärung

Ich erkläre hiermit an Eides Statt, dass ich die vorliegende Arbeit selbständig und ohne Benutzung anderer als der angegebenen Hilfsmittel angefertigt habe. Die aus fremden Quellen direkt oder indirekt übernommenen Gedanken sind als solche kenntlich gemacht. Die Arbeit wurde bisher in gleicher oder ähnlicher Form keiner anderen Prüfungsbehörde vorgelegt und auch noch nicht veröffentlicht.

Wien, am 15.05.2018

Unterschrift
(Maximilian-Zak Schaschl)

Acknowledgment

I would like to thank all those who contributed to the creation of this work.
First and foremost, my thanks go to Univ. Prof. Mag. Dr. Bernhard Grasemann, who made it possible for me to write this work and patiently left me the necessary freedom I needed. I would also like to express a very special thanks to Mag. Thomas Hofmann, who has always supported me and gave me the possibility to work on this thesis. Furthermore, I would like to thank Dipl. Ing. Roland Hochwartner, authorized representative of the Wopfing plant management, for permission to carry out this study in the Dürnbach quarry. Philipp Strauss (OMV Exploration and Production GmbH) introduced us to the regional geology of the Hohe Wand in general and shared his local observation in the Wopfinger quarry.
A big thank you to Sebastian Viehmann for proofreading this work and the generous coffee supply in his office. I would also like to thank my fellow students and friends. Marina Bauer, Sophie Kovacs, Johann Kuzel, Simon Niebergall, Gerhard Herda, Maximilian Rieder and Sebastian Pontz, which enriched my study time and made it precious. Special thanks go to Philipp Thalhofer, who always stood by me with help and advice, always motivated, inspired and had an open ear for me at all time. My thanks also go to Daniel Ritzinger for the provision of the measurement data, which he has collected in the course of his Master's thesis. Finally, I would like to thank my girlfriend and family. They always listened to my problems and concerns. Without their support and drive, I would never have been able to graduate.

Abstract

The technical developments in recent years have made it possible for Unmaned Aerial Vehicles (UAV´s) to become affordable and usable for mankind. This opens up a wide range of new opportunities for remote sensing, monitoring, media, and industry.

This master thesis presents a snapshot of the state of research in 2017 in 3D photogrammetry and its evaluation. In addition, the current commercially available drones were categorized and their advantages and disadvantages are briefly defined.

Vollgger et al. (2016) described the basics of the photographic system in view of the requirements for photogrammetric processing, while Dewez et al. (2016) (CloudCompare qFacets), Thiele et al. (2017) (CloudCompare qCompass) and Dr. Michael Roach (GeoVis 3D, AUSGEOL) developed plugins for existing, or stand-alone programs for evaluation purposes. The possibilities that currently exist with regard to the photogrammetric evaluation as well as the geological data acquisition of the resulting 3D models were carried out using the aforementioned freely available programs and plugins.

The open pit limestone quarry Dürnbach of Wopfinger Baumit GmbH was chosen as a reference example for this master thesis. By the use of a commercially available drone (DJI Mavic Pro), the abandoned lower section of the open pit mine was targeted to take a photoset. From the latter, a 3D model was created applying the photogrammetry software AgiSoft Photoscan. This model was subsequently evaluated in terms of geological data by the use of GeoVis 3D and CloudCompare with the aforementioned plugins. For comparison with traditional methods, the structural-geological mapping of the quarry, done by Daniel Ritzinger, have been used. As the results and comparisons show, the digital measurements are barely inferior to the hand-made measurements, but in some applications limited by the accuracy and richness of detail of the 3D model. This shows that the used drone and the applied methods are very accurate and promising and will often find application in the future.

The possibilities for geological data collection are very extensive, but this research and application area is still at its beginning (Carrivick et al., 2016). There are far-reaching opportunities for industry and the economy along with further research, because of the faster, safer and cheaper surveying possibilities. In the future, the use of drones and related applications will be indispensable and an important instrument of geology.

Zusammenfassung

Die technischen Entwicklungen in den letzten Jahren haben es ermöglicht, dass sogenannte UAV´s (Unmanned Aerial Vehicles) für jedermann erschwinglich und einsetzbar wurden. Dadurch bieten sich für die Wirtschaft und Industrie breitgefächerte neue Möglichkeiten zur Fernerkundung, Überwachung und den Medien.

Diese Masterarbeit stellt eine Momentaufnahme des Forschungsstandes 2017 in der 3D Photogrammetrie und deren Auswertung dar. Überdies wurden die aktuellen käuflich erhältlichen Drohnen kategorisiert und kurz in ihren Vor- und Nachteilen dargestellt.

Vollgger et al. (2016) beschrieb die Grundlagen der Fotoaufnahmesystematik in Rücksicht auf die Anforderungen an die photogrammetrische Verarbeitung, während Dewez et al. (2016) (CloudCompare qFacets), Thiele et al. (2017) (CloudCompare qCompass) und Dr. Michael Roach (GeoVis 3D, AUSGEOL) Plugins für vorhandene oder eigenständige Programme zur Auswertung entwickelten. Die Möglichkeiten, welche sich derzeit in Bezug auf die photogrammetrische Auswertung als auch die geologische Datenerfassung der daraus resultierenden 3D Modelle bieten, wurden mittels den zuvor genannten freierhältlichen Programmen durchgeführt und in ihren Abläufen behandelt.

Als Referenzbeispiel dieser Masterarbeit wurde der Tagebau Kalksteinbruch Dürnbach der Wopfinger Baumit GmbH gewählt. Der stillgelegte untere Abschnitt des Tagebaus wurde mittels einer kommerziell erhältlichen Drohne (DJI Mavic Pro) beflogen. Im Zuge dessen wurde ein Fotoset aufgenommen, aus welchem ein 3D Modell mittels der Photogrammetrie-Software AgiSoft Photoscan erstellt wurde. Dieses Modell wurde anschließend im Hinblick geologischer Daten mit den anfangs erwähnten Programmen ausgewertet. Zum Vergleich mit traditionellen Methoden, wurde auf die strukturgeologische Kartierung des Steinbruchs von Daniel Ritzinger zurückgegriffen. Wie die Ergebnisse und Vergleiche zeigen, sind die digitalen, den von Hand durchgeführten Messungen kaum unterlegen, jedoch in manchen Anwendungsfällen durch die Genauigkeit und den Detailreichtum des 3D Modells eingeschränkt. Dies zeigt das die eingesetzte Drohne und die angewandten Methoden sehr genau und vielversprechend sind und in Zukunft immer mehr Anwendung finden wird.

Die Möglichkeiten der geologischen Datensammlung sind sehr weitreichend, allerdings ist dieser Forschungs- und Anwendungsbereich noch an seinem Anfang (Carrivick et al., 2016).

Es bieten sich weitreichende Chancen für die Industrie und Wirtschaft einhergehend mit der weiteren Erforschung aufgrund der schnelleren, sichereren und günstigeren Landesaufnahme und weiteren Möglichkeiten. In Zukunft wird der Einsatz von Drohnen und den damit verbundenen Anwendungen unverzichtbar sein und ein wichtiges Instrument der Geologie darstellen.

1. Introduction

1.1. General

Due to the achievements made in the last few years a whole new research field and applications can be introduced by the use of UAV´s in the field of geology. The investigation of inaccessible or hardly accessible areas can now be performed much more easily and also orthophotos of small to middle large fields in high resolution is possible by little effort and low costs. The evolution of the hard- and software is so advanced that the handling of an UAV is conceivable for everybody. The knowledge and ability to fly a drone is very low these days, so the hardest part is to process and evaluate the gained data to gather the requested or needed results. The compilation of a 3D model is pretty simple by the use of 3D photogrammetry programs like AgiSoft Photoscan and others. Therefore, the complicated task is the further acquisition of data, which is for interest in the eye of a geologist. There is already some work done by Blistan et al., (2014), Bemis et al, (2014) and Vollgger et al., (2016) about the theory and methods behind the photo data acquisition and some implementations to CAD programs. At the present there are almost no “all in one” solutions available for geological purpose. The team around Photoscan is trying to extend their software for more analytical functions like volume calculations and Digital Elevation Models (DEM). One of the accessible solutions is ShapeMetriX provided by the company 3GSM which is in difference a high cost package consisting of the software and precisely calibrated camera systems. The goal of this thesis is to find an easy, free to low cost solution for the acquisition of geological data, which can be handled by every dedicated student or researcher. This includes the description of every step starting by the purchase of a certain UAV to the flight planning and the software, which can be used to gain specific geological data.

1.2. Digital Photogrammetry and Structure from Motion

Photogrammetry is the science of determining quantitative data out of analogue or digital photos. The easiest way to gather quantitative data would be the direct acquisition in the field like measuring distances and angles. Due to certain circumstances, it is often not possible to reach the area of interest, the region changed over the time, or even the relevant object is gone or destroyed. In this case, photogrammetry is the tool of choice, because if it is possible to determine the scale of a photo, it is possible to achieve the data looked for. (Linder, 2003). Structure

from Motion (SfM) is a form of the digital photogrammetry with the difference that the absolute camera positions are unknown. Due to overlapping picture-information, the camera position and orientation will be calculated by the SfM software. The result is a sparse point cloud, which then is getting refined by further "Multi View Stereo" (MVS) algorithms resulting in a dense point cloud. Therefore, the result is an unscaled and unreferenced 3D model. For scaling and georeferencing further position data are needed. This can be ensured by GPS metadata from the camera or so called Ground Control Points (GCP) in the area of interest where the exact GPS position is known.

1.2.1. Principe

Photogrammetry has similarities to solving a linear equation system. If there is only one photo with known scale, it is possible to get two-dimensional data like the length and width of an object. This might be enough for a few applications but in common the third coordinate, the height of an object is as important as the length and width. To attain the height component ("z"-coordinate) at least two pictures are needed, which are taken from different positions. A good example for the visualization of the three dimensions is the human sight. The eyes represent the "human-camera", which gather picture information from two different positions whereas the brain is the "human-workstation" and calculates the spatial pictures of the human sight. For the illustration, the case of aerial photogrammetry can be taken into account by looking at Figure 1. Every point on the surface has to be visible in two or more images. When all the geometric data of the position the photo is taken are known or can be computed, then it is possible to calculate the three-dimensional coordinates of the Point P. This is done by applying the ray equations and calculating their intersections. Due to this, it is easy possible to digitize the points of interest to get the information wanted like distances, angles, areas, etc. (Linder, 2003).

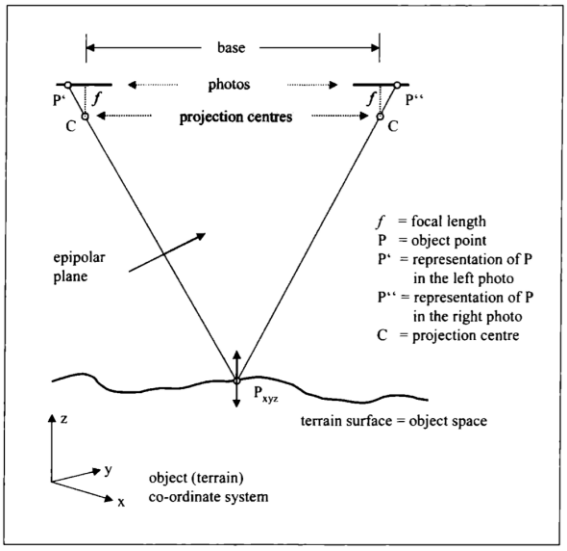

Figure 1: Photogrammetric principe. (Linder, 2003)

1.2.2. History

The photogrammetry evolved hand in hand with the development and introduction of new technical innovations and the progress in science. There are four major development steps

followed by the introduction of their fundamental technologies: the photography, aircrafts, invention of computers and their further development.

Due to the invention of photography by Daguerre and Niepce in 1839 the first generation of photogrammetry was introduced in the 19th century on terrestrial and balloon based applications.

The analogue photogrammetry, the second generation, was introduced by the invention of the stereo plotter by Orel in 1908. The technology became widely available in the science and established itself as an efficient monitoring and mapping tool. The third generation has arrived with the advent of computers and is described as analytical photogrammetry. Due to the analytical potential because of the computing power, the first applications for triangulation purposes were quickly developed. In the late 1960s, computer-programs were introduced which resulted in a 10 times higher accuracy of the triangulation of aerial photos.

With the modern digital age, the fourth generation of photogrammetry, the so-called digital photogrammetry, has been introduced. In recent years, much research and development has been done to make digital photogrammetry easy and available to everyone. With digital cameras, which meanwhile everyone carries in their pockets in the form of a smartphone and uncomplicated, powerful software solutions, photogrammetry has reached everyday life (Schenk, 2005).

1.2.3. Field of Application

The bandwidth where photogrammetric applications are used is developing very fast and is getting even broader with the time. It ranges from the documentation of buildings and damages or the survey of crash tests to digital models of outcrops. Archaeologist use it for the fast conception of oversight maps and the documentation of archaeological sites. A very big field of use is the digitalization of objects like prototypes in the engineering branch or the capture of a hand specimen. In the origin, photogrammetry was mostly used in the geodesy for measuring purposes and the generation of rectified orthophotos.

Therefore, in the latter paragraph the most interesting applications for geologists is the three-dimensional digitalization of outcrops and the fast creation of orthophotos. In comparison to other digital survey methods, one of the biggest advantages of photogrammetric methods is that there is no special equipment needed. A camera, a PC and photogrammetric software is the basic equipment and apart from the software, available to everyone. Compared to other

methods, this is a huge advantage as there are no high costs, and the operation does not necessarily require specially trained personnel. In the following table from Carrivick et al. (2016), the different advantages and disadvantages of the individual digital survey methods are shown:

Table 2.3 Summary of properties and pros and cons of different digital survey methods.

Survey equipment and workflow	Typical spatial extent (km)/ typical spatial resolution (pt.m²)	Possible data acquisition rate (points per hour)	Possible 3D point accuracy (m)	Advantages	Disadvantages
TS	0.1–1.0/0.1–5.0	Hundreds	<0.001	Low cost Accurate	Line of sight required Low productivity Accuracy decreases with distance from base
dGPS	2.4–1.0/0.1–5.0	Thousands	0.005	High accuracy Range of methods have been developed to suit different surveying requirements Line of sight not required	High cost Some methods have low productivity Lock on 6+ satellites required
Photogrammetry	5.0–50.0/ 0.5–10.0	Tens of thousands	0.5	High productivity Once set up, no operator required Continuous information can be captured	Low resolution Equipment must be left in position for long periods of time (depending on survey) and may be vandalised or damaged Does not work in fog, mist, etc.
ALS	5.0–100.0/ 0.2–10.0	Millions	0.2	High productivity Can be used during the night Airborne LiDAR can survey areas that are difficult to access Not affected by vegetation cover	Very high cost Resolution may be insufficient to measure small changes Systematic errors on some landforms
TLS	0.01–5.0/ 100–10,000	Millions	0.05	High accuracy	Unable to capture all aspects of complex topographies (depending on equipment positioning)
SfM	0.01–1.0/ 1–10,000	Millions	0.01–0.2	Cheap Fast Method is independent of spatial scale	Reproducibility? Reliability?

Advantages and disadvantages are adapted with permission from Young (2013). Extent and resolution values are from figure 12 in Bangen et al. (2014).

Figure 2: Comparison of different digital survey methods.

1.3. UAV's

1.3.1. General

The abbreviation UAV represents the collective term for all ground controlled or autonomously flying aircraft. This category includes fixed wing aircraft, helicopters, multicopters

and airships, which are subject to scientific, economic, military, but also private purposes. UAVs are also widely known as drones. However, this term is often associated with negative characteristics, since it is mostly used in German-speaking countries in connection with military purposes. It should be noted that a UAV is not used in the sense of flying, as with remote-controlled aircraft models, but as a platform for various sensors and different survey tasks.
As a result, UAVs are subject to more and more legal requirements and restrictions, which are controlled and licensed in Austria by the Austro Control, Austrian Civil Aviation GmbH (ACG). Depending on the field of application and airspace, different legal requirements apply to the aircraft and the pilot. This is to ensure that the technical safety of the UAV and the capabilities of the pilot meet the application requirements.

1.3.2. Development

Remote-controlled model aircraft made their entry already in the early 1950s, the technology was still very prone to failure at the time and very expensive. Only with advancing technology, the radio links became safer and remote-controlled models more powerful. The area experienced a quantum leap with the emergence of modern power electronics, sensors, microelectronics and battery technologies. With these prerequisites, it was possible to develop motors, radio remote controls and flight controllers, which allow almost everybody to control a UAV. Ten to fifteen years ago, remote-controlled UAVs were still cost-intensive and highly specialized niche products. Meanwhile, so-called photo drones have been introduced almost everywhere and are affordable and usable for everyone. A drone comparable to a current mid-range consumer drone for ~800 € would have cost at least 10 times as much in the past.

1.3.3. State of the art

Current UAVs offer a variety of sensors and software features, which make the data acquisition and operation for non-specialized users possible. The basic equipment now includes position sensors, acceleration sensors, 3-axis magnetic field sensors, GPS and / or GLONASS sensors, barometers and, increasingly, stereo cameras for obstacle detection. Only the operating software allows a smooth interaction of this abundance of sensors and offers features that enable, for example, autonomous flying and the information for the pilot about the flight data. Normally, the drone is operated via a remote control, which are usually equipped with a holder for smartphones or tablets. On the latter devices, the flight data and the live video of the camera on board the aircraft are displayed, the settings and the flight parameters edited. In some software solutions, a so-called "ground station" is additionally used. This is usually a laptop, with the help of which complex flight tasks are planned and monitored.

1.3.4. Applications

Due to the aforementioned developments, the areas of application for UAV´s are becoming more diversified. In the past, they were largely military purposes such as airborne reconnaissance and later reserved as tactical weapons for air-to-ground attacks. Today's applications fall into areas such as:

Agriculture:	UAVs with multispectral cameras to assess the vitality of plants
Documentation:	Assessment of various structures in hard-to-reach places or areas that pose a significant security risk
Logistics:	Large mail-order companies like Amazon carry out projects to deliver goods to the end customer as quickly as possible using drones
Security:	For the investigation of disaster areas, forest fires or for the search of criminal persons
Media:	Drones are being used for landscape photography and film productions
Private users:	Photography and fun flying
Geology:	Easy creation of orthophotos, remote sensing of hard-to-reach areas such as rock walls, 3D outcrops and their evaluation

1.3.5. Available UAV´s

Global leader in the consumer drone market is undisputed DJI, revolutionizing the drone world with the introduction of the Phantom 1. Today there are a lot of supplier for consumer to professional UAV´s like DJI, Parrot, 3DR, Lockheed Martin, Yuneec to name the most prominent manufacturers. Nowadays there is almost no difference according to the features of the available drones which leads to a very wide spread market to choose from. The question is what field of application and in which terrain the drone should operate. For summary, the drones can be differed into three groups:

Small and mobile UAV´s

Drones like the DJI Mavic, Yuneec Breeze or some Parrot models are predestined for the operation in impassable areas. Due to their lightweight and small dimensions, it is an ease to carry them by yourself at long hikes or difficult ascents. The packing size allows them to be carried in small pouches or in every backpack. The price of such a small drone starts at about 300€ up to 1200€. In addition, the landing space required is a certain point where the advantages of those small UAV´s take effect. Only a ~50x50cm flat spot is necessary to initialize

the drone, take off safely and land manually. Even if the wind is too gusty or strong or if the operator moved with the drone due to a better sight and no safe landing is likely, it is possible to catch the vehicle by hand (note: this is not recommended and can lead to injuries or a damaged UAV by a failed catch).

These positive aspects do not come alone and so several handicaps exist, which should be taken into account and considered by the decision. Affected by the lightweight and dimensions some throwbacks concerning the camera equipment and the wind sturdiness have to be accepted. Smaller camera sensors and higher apertures what means less light can be captured, which lead to lower quality photosets. Also mostly proprietary camera systems are used which prevents individual customization. A specific factor is the wind sturdiness, which is influenced by the power of the aircraft and as a rough guide, the heavier the aircraft, the better it can withstand windy conditions due to its inertia.

Advantages	Disadvantages
Mobile	Lack of camera quality / options
Lightweight	Vulnerable to bad weather conditions
Low cost	
Easy to operate	
Small take off / landing space required	

Table 1: Summarized advantages and disadvantages of small and mobile UAV´s.

Middle class UAV´s

This class includes "all-round" models like the DJI Phantom and the Yuneec Typhoon series. The cost of drones in this category is around 800€ to 2000€. Due to their size and performance, they can carry both larger and better cameras as well as more sensors. As a result, the photo quality and handling is better and increases security. The wind compatibility is increased, but the disadvantages come into play. An own transport backpacks is needed, which makes the accessibility of difficult terrain as well as long journeys and ascents difficult. At the same time, the required take-off and landing site is more demanding and it is no longer justifiable to catch the drone.

Advantages	Disadvantages
Semi-professional camera quality	Higher weight
Resistant to windy weather conditions	Higher cost
Still mobile	Higher noise level
More sensors	
Easy to operate	

Table 2: Summarized advantages and disadvantages of middle-class UAV´s.

High-end surveillance UAV´s

The UAV´s in this category, such as the DJI Inspire, S800, S1000 or the Matrice platform as well as other industrially used drones, are mostly only to be operated with special ascent requirements, insurance and special requests for the drone operator. This is governed by the AustroControl, which also grants the authorizations. The price range starts at around 3500 € with no limits to the top. Both, proprietary camera systems as DJI offers, also other camera gimbals for a variety of cameras such as small compact cameras up to DSLR or multi-spectral cameras can be installed. Furthermore, there are various possibilities to customize or supplement these platforms. Thus, not only a photo camera, but also additional sensors such as the already mentioned multispectral cameras, laser scanners, infrared cameras or high-precision positioning systems such as the DJI D-RTK GNSS, which enables positioning accuracies in the cm range, can be installed. Due to this wealth of possibilities, which goes hand in hand with a significantly higher weight and dimensions, these UAVs are only to be used for quasi-stationary operation. It is almost inevitable that the application area can be reached with a vehicle, since not only the aircraft itself but also often additional equipment such as laptops, power stations for charging purpose and desks are needed. Furthermore, there is the necessity for a second drone operator to divide the flight and surveillance tasks.

Advantages	Disadvantages
Professional camera quality	Immobile
Resistant to windy weather conditions	Very high cost
Very broad field of application	High noise level
Long flight times	Need of ascent requirements
Precise positioning	Additional equipment
	Specialized operators needed

Table 3: Summarized advantages and disadvantages of high-end UAV´s.

1.3.6. DJI Mavic

The choice fell on the DJI Mavic Pro due to the before mentioned advantages. The main focus was to purchase a drone that is very lightweight and mobile for the use in difficult terrain, easy to handle and still has a descent camera. It is a drone of the latest generation and offers far-reaching applications due to its

Figure 3: DJI Mavic unfolded. (DJI, 2017)

small dimensions and the comprehensive sensor technology and software. The UAV has a radio range of up to 4 km and a HD video transmission with a latency of 160 ms under perfect conditions. The arms and propellers are foldable, which leads to a very small packing size. The maximum flight time is 27 minutes, the maximum flight speed is 65 km/h (sports mode). The stabilization takes place by position, acceleration, compass, ultrasonic, barometric and GPS / GLONASS sensors. Furthermore, the drone has a stereo camera pointing in flight direction for the obstacle avoidance (OA) and a bottom stereo camera to improve positioning at low altitudes (Vision Positioning System / VPS), more accurate home tracking and terrain tracking. The camera system is stabilized by means of a 3-axis gimbal and thus enables perfect shots even in gusty weather conditions. The camera has a resolution of 12MP, a field of view (FOV) of 78.8 °, a focal length of 28 mm (equivalent to 35 mm format, real 4,91 mm), an aperture of f/2.2 and a lens distortion of less than 1.5 %.

The remote control has a folding mechanism, which allows in the unfolded state, the attachment of the smartphone. The antennas are also hinged, where the alignment of them is of essential importance for the transmission range of the transmitter. The remote control is equipped with an LCD display, which can display the most important flight data and warnings.

1.4. Regional Geology

1.4.1. General

The sampled quarry of Dürnbach is located in lower Austria near Hohe Wand (Northern Calcareous Alps, NCA Fig. 4, 5). The NCA reach from the Alpenrheintal to the western border of the southern Vienna basin and extend in the subsurface to the Carpathians. The NCA are composed of mostly calcareous sediment layers formed in different sedimentation zones that reach from Permian to Palaeocene age. The stratigraphic thickness reaches up to 8km and is separated into different nappe systems (Wessely, 2006).

The NCA roughly strike from the west to the east and forms in a cross section an up to 40 km wide and 500 km long fold-and-thrust belt. The highest peaks in the western and central part reach up to 3000 m (Parseierspitze, 3036 m) and in the eastern part up to 2000 m (Schneeberg, 2076 m) (Mandl, 2000).

The deposition started in the Permian with evaporites and continental to shallow marine siliciclastics on the Variscan basement till the end of the Early Triassic when carbonatic sediments became prevailing. In the Middle to Late Triassic, platform carbonates are dominant and influenced by terrigenous sediments in the Early Carnian and Late Norian originating from the European hinterland. The Hallstatt facies is composed of pelagic Limestones, deposited on

the distal deeper shelf and was affected by synsedimentary diapirism of the Permian evaporites. The NCA together with the Grauwackenzone has been sheared of the basement and tectonically lie over the Penninic Rhenodanubian Flysch Nappes. Due to the opening of the Vienna Basin and strongly influenced by the subducted Variscan Basement the strike of the tectonic units changes to an NE-SW direction close to the western margin of the Vienna Basin (Mandl, 2000; Wessely, 2006).

1.4.2. Tectonic

The NCA are divided into three main tectonic units: Bajuvarikum, Tirolikum and Juvavikum. Different minor units are summarized in the main units:

Main Unit	Minor Units
lower Bajuvarikum	Frankenfelser Nappe
upper Bajuvarikum	Lunzer Nappe
upper Bajuvarikum – Tirolikum	Sulzbach Nappe
Tirolikum	Reisalpen-, Unterberg-, Göller-Nappe
Juvavikum	Schneeberg-, Mürzalpen-, Hallstätter-Nappe

Table 4: Distribution of the minor units.

This nappe complex was formed due to several stages of folding and thrusting from the Late Jurassic to Tertiary times. The deformation lead to the overthrust contact with the Rhenodanubian Flysch Zone in the north and with the Variscan basement in the south.
The Bajuvarik nappes build the frontal northern part of the NCA, which are characterized by narrow synclines and anticlines. Those are overthrusted on their southern part by the Tyrolik nappes. Due to the dolomitic lithology of the Tyrolik nappes internal thrusting and faulting is dominant and only minor folding occurs. The uppermost tectonic unit is built by the Juvavik nappes, which overly the Tyrolik unit and show in difference to the most parts of the NCA a considerable thermal overprint in some areas.
Rifting and spreading of the Tethys ocean formed the NCA depositional area, which was a passive continental margin during the Permo-Triassic. The area adjacent to the NCA and the Western Carpathians also known as the "Hallstatt Meliata Ocean", was closed in the course of the Jurassic period. Contemporaneous the Austroalpine realm became separated from the European hinterland, which was the birth of the Penninic ocean linked with the opening of the central Atlantic ocean, due to a major transform fault. The first displacements of the Juvavic nappes was caused by compressional tectonics at the same period.

In the Cretaceous subduction processes at the southern margin of the Penninic ocean led to its closure and was accompanied by crustal shortening within the Austroalpine crystalline basement and nappe movements.

Clastic sediments of the Gosau Group were deposited on the NCA nappe stacks in the Late Cretacious. The Rhenodanubian Flysch Zone became partly overthrusted and deformed in the Late Eocene by the NCA nappes. By several drillings with depths between 3000 – 6000 m reaching the basement, all units of the overthrusted Molasse Zone, Flysch Zone and the European foreland were penetrated. This proved the large-scale thrusts of the NCA over this zones. The NCA nappe complex was also affected by the uplifting processes of the Eastern Alps caused by large strike-slip movements like the sinistral Salzach-Ennstal fault system (Mandl, 2000).

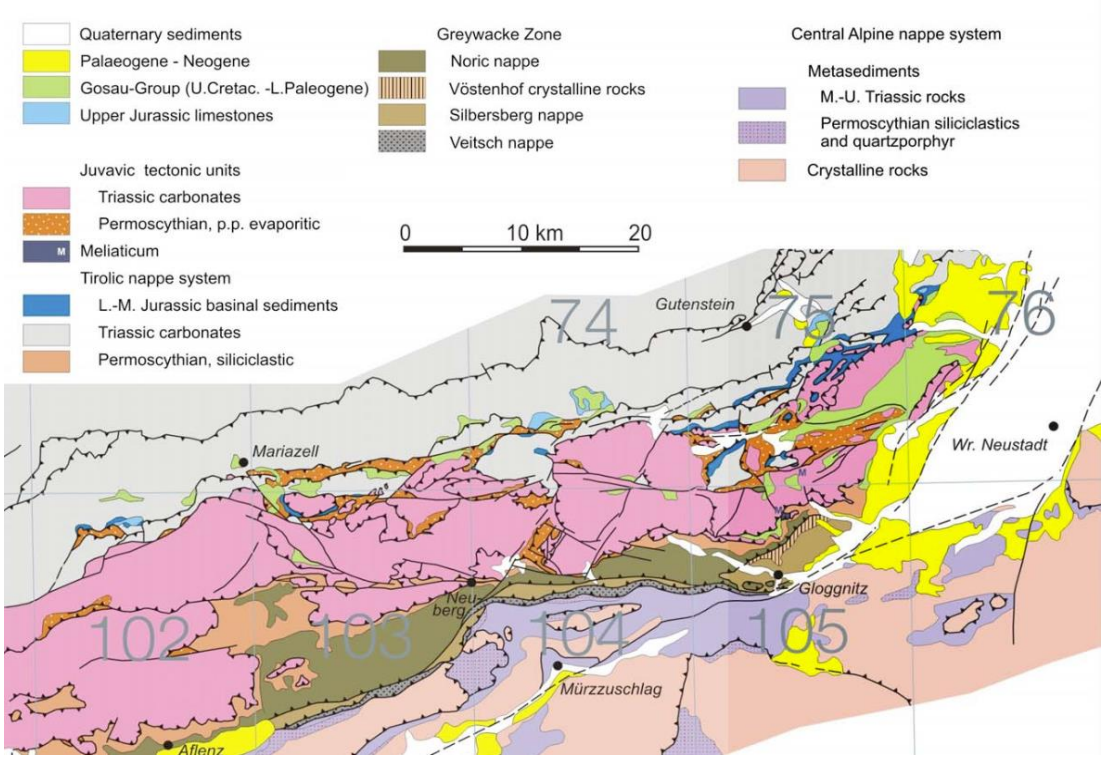

Figure 4: Tectonic overview of the eastern NCA. (Mandl, 2000)

1.4.3. Quarry Dürnbach

The quarry is near the Hohe Wand and about 16km in the west of Wiener Neustadt located nearby the village of Waldegg (Fig. 5). According to the database of the Austrian geological survey (Geologische Bundesanstalt, GBA) the quarry has the file number 075/101. The mine is in operation since 1967 (Wopfinger Rohstoffe) where two main areas can be differentiated: the active part where the limestone is produced and the older part in the lower section of the quarry where no active production takes place. The latter section is the area, which was investigated in course of this thesis.

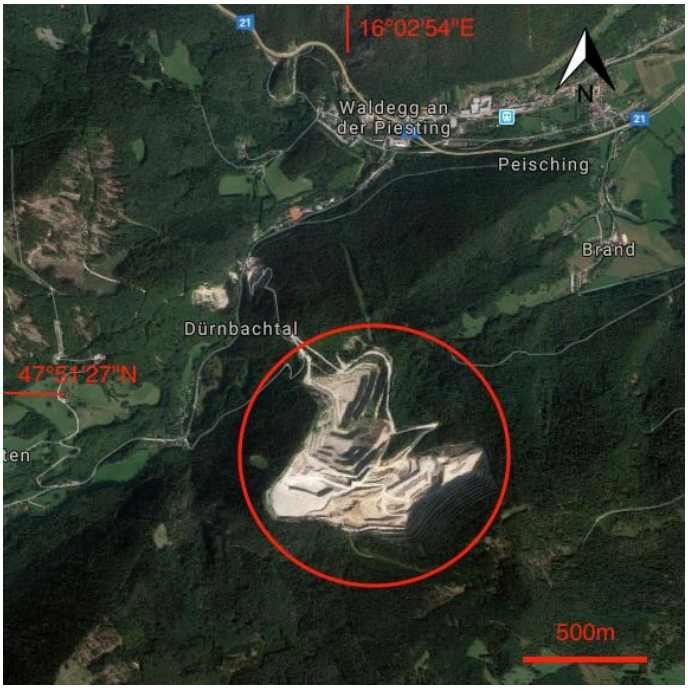

Figure 5: Satellitephoto of the Quarry Dürnbach.

1.4.4. Lithology

The main lithology in this area is the so called Dachsteinkalk (Fig. 6) which is named after its type locality the Dachstein–Massif. The age of the Dachsteinkalk correlates to the upper Triassic (Tuvalium ca. 219 – Rhätium 199,6 Ma (Piller et al. 2004) and can be separated into the Bankkalk and the Riffkalk due to its building facies. In the main-sedimentation period, the thickness of the deposited limestone reached up to 1 km. The exposed Dachsteinkalk in the quarry associates to a reef near lagoonal facies deposited during the upper Nor to Rhätium (Summesberger, 1991).

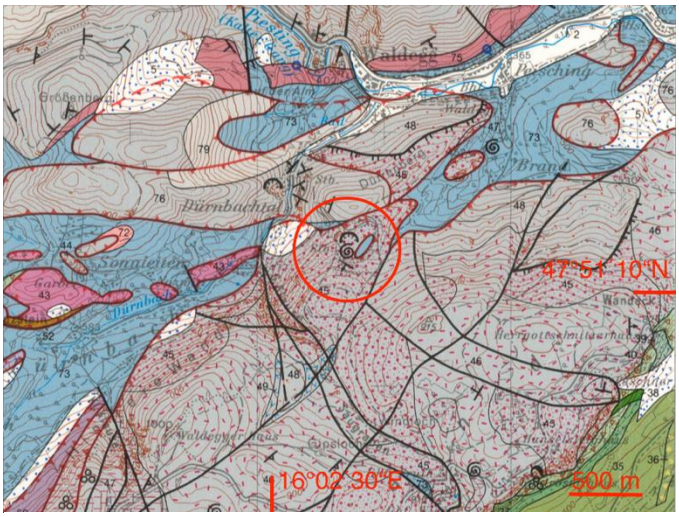

Figure 6: Geological map of the quarry and the surroundig area. (Summesberger, 1991)

Typical for this pit is the reddish colour of the Limestone which is caused by terrigenous deposits and sometimes macrofossils like Megalodonts can be found. In addition, a characteristic feature are sedimentation sequences following the so called Lofer Cycle, described by Tollmann (1976). The cycles are grouped in three stages (Fig. 7):

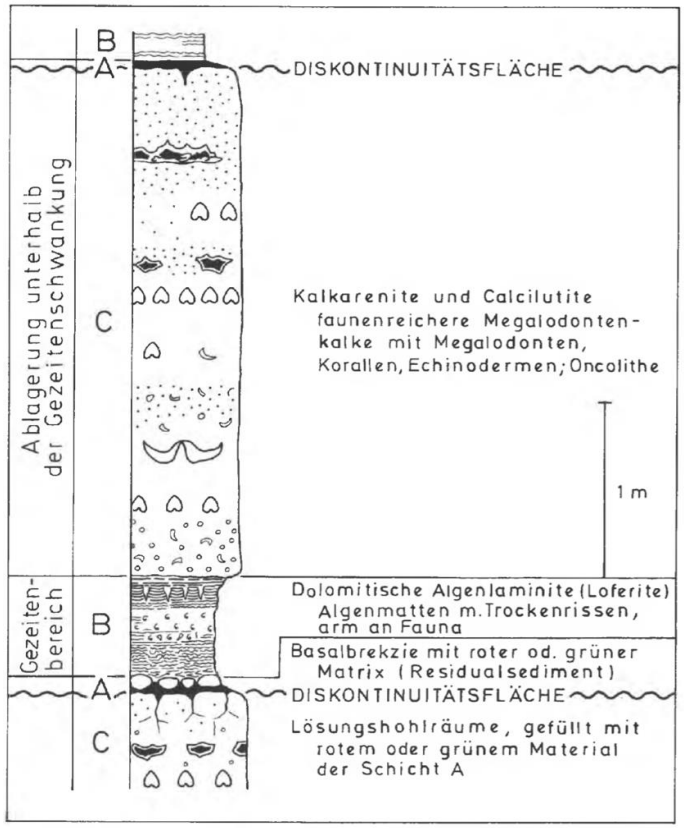

Figure 7: Ideal sequence of a "Lofer Cycle". (Tollmann, 1976)

A: Discontinuity surface due to an emerge above the sea level, caused by erosion which lead to a thin section of red, green or greyish clay with reworked limestone debris.

B: 10 – 50cm thick layer of so called Loferites which are the result of rhythmically changing calcitic - dolomitic algae mats. These mats contain characteristic pore cavities, which are filled with Calcite ("birds eyes").

C: A few meter-thick layer of Megalodont-Limestone with a fine grained matrix. The fauna contains Megalodonts, Gastropods, Echinoderms and higher algae deposited under a subtidal environment with persistent water coverage.

In certain areas of the quarry there is also Lias-Fleckenmergel exposed which is due to the tectonic interaction of the Göller Nappe with the Juvavic blocks.

2. Methods

2.1. General

The most important point by the planning of a 3D model is to know what information should be received. Therefore, the first step is to create a list with the features that should be extracted from the model. Those can be data like the thickness of a bedding, volume of a rock pile, plunge and dip of a certain plane, the sampling of orthophotos, etc. In every case, it is essential to know what ground sampling distance (1) (GSD) can be achieved with the used equipment. This describes the distance between pixels measured on the ground. It has an inverse relation to the resolution of the model. To calculate the GSD following equation and specifications are needed (Vollgger et al., 2016):

$$GSD = \frac{AGL \times W_{Sensor}}{W_{image} \times f} \qquad (1)$$

AGL: height above ground level [m]
W_{Sensor}: physical width of the sensor [mm]
W_{image}: width of the picture [pixels]
f: (real) focal length [mm]

For example, it is easy to get a high-resolution model (low GSD) of a boulder where a large set of photos are taken from a short distance. In contrast if the goal is to create a model of a large quarry the resolution will be lower (higher GSD) because of hardware limitations due to the high workload for the PC workstation and the complex flight strategy and duration. This is an individual limitation, which depends on the computing capacity and the ability to handle extremely detail rich models and orthophotos and the effort that has to be operated. In general, it can be said that the bigger the area to investigate the lower detailed is the model. Another point, which has to be taken into account, is the topography of the area, which should be captured. Depending on that, different strategies are needed to create a photoset. Generally, the purpose of the planning is to achieve a set of overlapping photos with a certain distance to the object / area, which is defined by the ground resolution that should be attained. In conclusion, the following points have to be determined (Nex et al., 2014):

Ground Sampling Distance (GSD)

Which details should be displayed?

Properties to be observed

Planes, Volumes, Orthophotos, etc.

Effort, which has to be taken into account

Fieldwork, Computational capacity, post processing

To achieve a sufficient overlap of the photos taken, a few parameters have to be calculated. Important parameters are the shutter interval $T_{interval}$ (2), the spacing between the parallel flight lines $S_{flightline}$ (3) and the motion blur MB (4) if the UAV is not stationary while image capturing.

So following equations are introduced after Vollgger et al. (2016):

$$T_{interval} = \frac{H_{image} \times GSD}{V_{horizontal}} \times \frac{100 - OL_{forward}}{100} \quad (2)$$

$$S_{flightline} = GSD \times W_{image} \times \frac{100 - OL_{side}}{100} \quad (3)$$

$$MB = \frac{V_{horizontal} \times T_{shutter}}{GSD} \quad (4)$$

$T_{intervall}$: time between photo capture [s]

H_{image}: image height [pixels]

$V_{horizontal}$: horizontal flight speed [m/s]

$OL_{forward}$: image overlap in flight direction [%]

$S_{flightline}$: spacing between the flight lines [m]

W_{image}: image width [pixels]

OL_{side}: image overlap perpendicular to flight direction [%]

MB: motion blur [pixels]

$T_{shutter}$: camera exposure time [s]

Agisoft is recommending in their user manual following overlap: “In case of aerial photography the overlap requirement can be put in the following figures: 60% of side overlap + 80% of forward overlap.“ (Agisoft User Manual p.8)

2.2. Mission planning

A good planning is the first step to a detailed and consistent 3D model. The key is to get the right amount of photos shot from the angles and positions required to fulfil the demands of the

photogrammetry software. This is inevitable to build a complete and gapless model without the necessity of any extra effort like a second photo set.

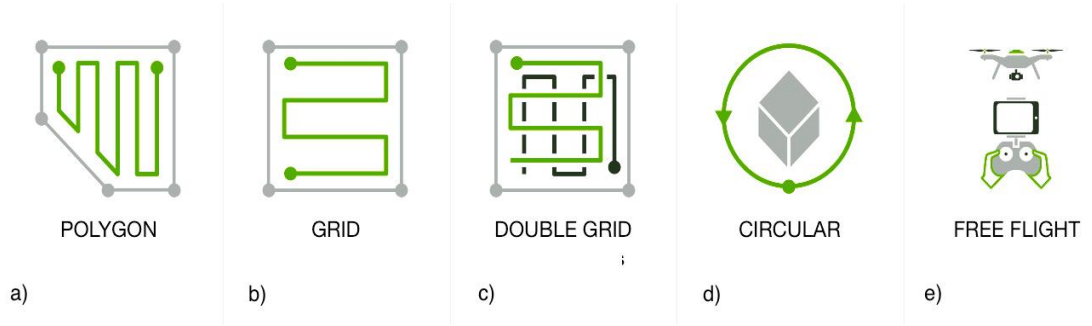

Figure 8: The most common flight strategies. (Pix4D App)

The first step is to know what data has to be acquired because the different flight strategies depend on this fact. The second step is to know the topography of the area to investigate. The third step is the determination of the GSD and the scale of the area to be flown.
With the interaction of the previous described facts, the right flight strategy can be derived. There are different options to accomplish the flight task. Depending on the drone, flight controller and the software to be used the flight strategy has to be flown manually, semi-autonomous or full autonomous.

In Figure 8 the different flight strategies are shown which depend on the different tasks that should be solved. Goal of these different flight paths is to capture photos with a good orientation to the object or ground surface. The more perpendicular in respect to the surface the better the alignment and spatial resolution.
Figure 8 a) and b) show the simplest schemes to collect an area covering photoset. These types are preferable for the creation of orthophotos or 3D models with a flat topography. The camera mostly points in nadir direction for flat areas and orthophotos or with an angle of about 30° - 60° for 3D model data collection. The latter is to generate a better spatial resolution, which helps to generate a more accurate model according to height precision. Attention has to be paid on the alignment of the flight grid to the topography. For example, to gather a data set of a dune, which has an elongated propagation from E – W, the parallel main flightpaths should be aligned in N – S direction to receive proper positioned photos.
A double grid flight strategy (Figure 8 c) is in point the most time consuming but the most accurate way to go for slightly complex topographies like quarries or steeper outcrops.
For homogenous outcrops, stockpiles or a summit, circular flight missions sometimes also called “Point of Interest (POI)” can be a very practical option especially in combination with different flight radiuses and flight heights (Figure 8 d).

In very complex terrain, overhanging or at least vertical walls there is still the need of controlling the drone manually. For this case, it is an advantage when the drone-operator brings some advanced flying skills to accomplish the difficult flying task. Under these circumstances, the pilot has to do the work, which normally does a third party application like Pix4D. Distances, overlap and flight time management are the parameters, which have to be taken into account by flying manually (Figure 8 e).

2.3. Software Applications

2.3.1. Flight-Software-Applications

Software applications can save a lot of workload for the pilot. Beginning by the "stock-apps" of DJI, Parrot, etc. a vast of third-party applications have been developed in the last years. First of all, there has to be a differentiation done between mobile applications and desktop applications commonly called as "Ground Station". In general, these programs have the same purpose, to make the flight planning easier and to automate the flight task. In Table 5 a list of now available apps is shown (no guarantee for completeness):

Mobile Apps	**Desktop Apps**
Pix4D Capture	UgCS Desktop
Litschi	DJI PC Ground Station
Autopilot	QGroundControl
DJI Go 4	
DroneDeploy	
MapPilot	

Table 5: The most prominent flight software applications.

Which one to choose is a question of what tasks have to be accomplished with the drone.
Mainly speaking the mobile apps do not differ very much, it is more a decision between a few little advantages or disadvantages to each other. For example, some applications do not have an automatic "start where stopped" function, which is useful during long missions. Pix4D is in this case very comfortable and does also all the calculation of the GSD, flightpath distances, etc. directly when setting parameters like camera angle, photo overlap, flight location and strategy.
In some special cases like flying inside a quarry, one of the main problems is the lack of height information. For example, a pit with a various number of levels, which differentiate in height,

geometry and area, is a difficult task when the resolution of the model should stay constant. That is the point where professional Ground Station applications like UgCS take effect. This for instance is much more powerful in kind of setting flightpaths, parameters and in addition, it is able to create 3D flight strategies. To enable this feature, a digital elevation model (DEM) which is available due to former surveying work or is generated by a foregoing reconnaissance flight is needed. The price tag for these advantages is the need of a laptop in the field and the price of the software itself.

2.3.2. Photo processing

When all the fieldwork is completed, the pre-processing of the data has to be done. The effort to be taken into account for the photo processing depends very much on the weather conditions during the photo acquisition and the file format the pictures were captured. The most common formats for digital photos are the JPEG and the DNG RAW format.

Pro and contra of the JPEG file format is the compression and ongoing with this the loss of information. In addition, the photo is processed in the camera by tweaking the photo parameters like brightness, contrast, etc. to get a nice picture. If these parameters vary due to changing outer factors like the lighting, focus, etc., it will result in a heterogeneous photo set. This is negligible if the weather conditions are constant and the main goal of the 3D model is in a quantitative manner.

In contrast to the latter, the DNG format does no compression or processing to the picture information so the data is “raw” and the whole potential of after processing software can be used. Disadvantage is the data size of these uncompressed photos, which leads to a higher demand of computing capacity and fast data storages.

There are many software applications for the processing of RAW images that vary in the scale of editing possibilities and grade of automation. A few examples are Adobe Photoshop, Adobe Lightroom, RAWTherapee and IrfanView.

In conclusion, the choice of the file format depends on the environmental parameters, the effort for the post processing and the requirements to the model.

2.3.3. Photogrammetric Software AgiSoft Photoscan

PhotoScan is one of the most common semi-professional photogrammetric software at the moment. It is an image based 3D modelling application based on the latest photogrammetric technologies to achieve high quality spatial models out of still photos.

To calculate the model, it is needed to load the post processed photo set to PhotoScan which should be revised of blurry or unnecessary photos to ensure the quality and save computing resources. After that the first computational step can be started:

- Photo Alignment
  At this step the software searches for matching points in the photos, calculates the camera positions and as a result a sparse point cloud is generated and an oversight of the camera positions.

- Dense Point Cloud
  In the second step, the dense point cloud will be calculated by using the prior defined camera positions. Every point has X, Y, Z coordinates and colour information (RGB). The density of the cloud depends on the amount of photos and the parameters set in the "Building Dense Point Cloud" context menu.
  After that, it is already possible to export the point cloud for further use in point cloud processing software applications.

- Mesh Build
  Due to the dense (or sparse) point cloud, PhotoScan derives a mesh representing the surface of the object. In common, the more points (higher density) the more polygons can be calculated, the more precise the surface will match the real surface. Additional operations can be done after the mesh build like a decimation of polygons, closing holes or smoothing the surface.

- Texture
  The final step is the texturisation of the mesh by matching pixel-areas through different projection types of the image information. Now the model can be exported as Google Earth .kmz file, 3D .pdf file, AutoCAD .dxf file, and many others, build a DEM or generate an orthomosaic.

It is possible to geo-reference the model by the use of Ground Control Points (GCP´s) during the photo acquisition for applications like surveying tasks. As the study from Tonkin et al.,(2016) shows a GCP count of at least four is recommended. It is demonstrated in this study by 16 individual DSM´s with 3 to 101 GCP´s that the vertical precision can reach <0,09 m.

If the camera has a build-in GPS module the photos can be geotagged so this metadata can be further used for a „low precision“ geo-referencing.

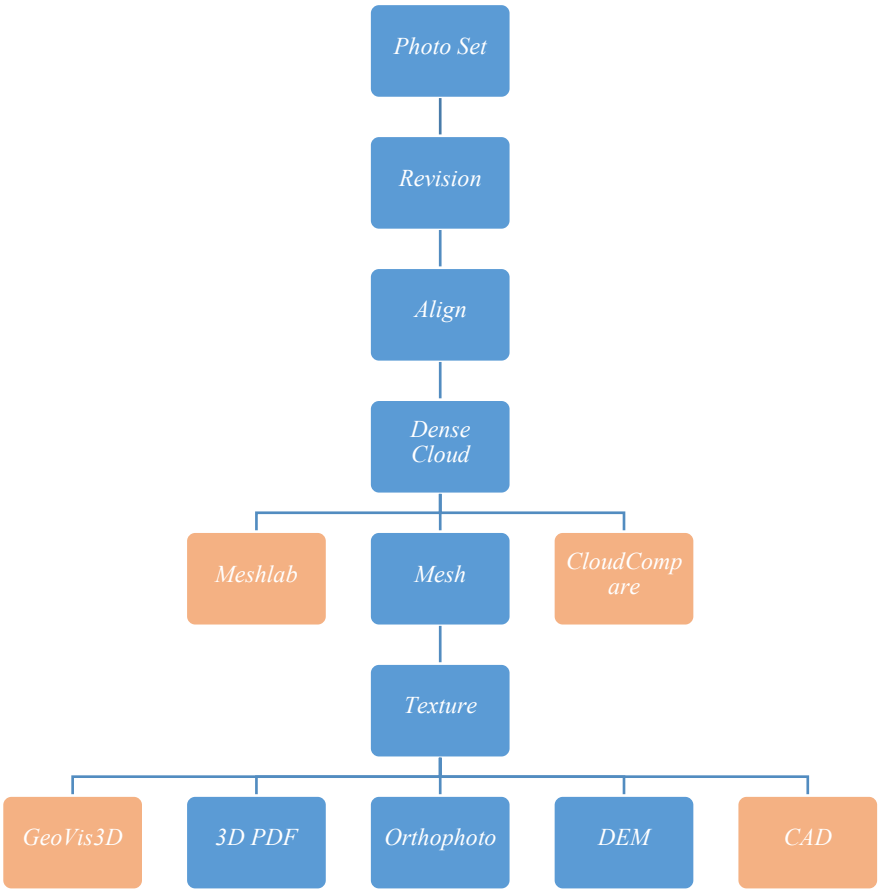

Table 6: Flowchart of the Photoscan workflow and the different output levels.

In summary AgiSoft PhotoScan is a very easy to handle application that needs low effort to get good results. The user manual provided on the homepage of AgiSoft is a very good assistance when doing the first attempts but like so often it is “learning by doing” and gather experience.

2.3.4. Data Evaluation Software

A vast amount of applications is available to compare, edit, transform and evaluate point clouds, which are the end product of AgiSoft. Not every program uses those point clouds, for example, GeoVis3D uses .kmz files, which are compressed .kml data that contain geo information like vectors, place marks and others. In the following chapters the possibilities, advantages and disadvantages of the different software solutions will be described and explained.

2.3.4.1. GeoVis3D

This software was developed under the lead of Dr. Michael Roach from the University of Tasmania for the AUSGEOL project. GeoVis3D is working on Windows and Mac using .kmz files created as output of a PhotoScan project and is based on a gaming physic engine. The usability is very easy and two Tutorial videos can be found on YouTube made by Dr. Roach.

User Interface

The interface is designed very clearly with the 3D model in the main area, on the right-hand side a stereoplot and a list with dip and strike data of the measured features can be found. In the lower area, there are two dropdown menus for the "Sample Mode" and "Feature Type" beside a field, which provides information about the quality of the measured plane and orientation data.

Workflow

First the model hast to be exported in the right format. The model can be exported from AgiSoft PhotoScan by clicking on File → Export model. The format .kmz for file type has to be chosen and then exported. GeoVis 3D can be downloaded from http://www.ausgeol.org/geovis3d/ . First the described installation advises belonging to the used operating system have to be mentioned. The settings for the screen resolution and the graphic quality have to be selected now. Click "Play!".

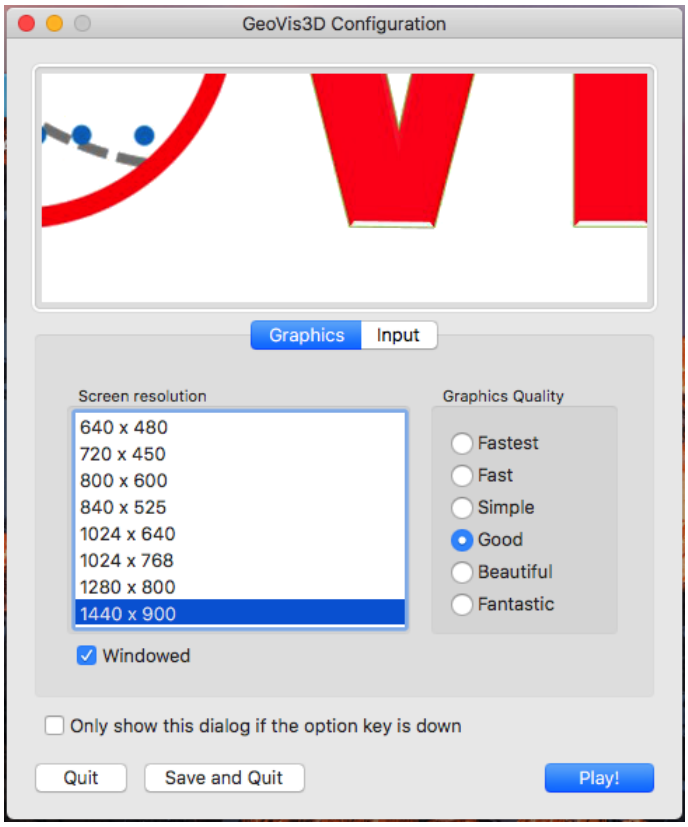

Figure 9: GeoVis 3D configuration window.

A new session can be started by clicking on the equally named item and a menu will open to choose the .kmz file to be edited. After the file is chosen, it can be loaded by clicking on “Open”. It will take a few seconds, depending on the size of the model, to be loaded (Fig. 10).

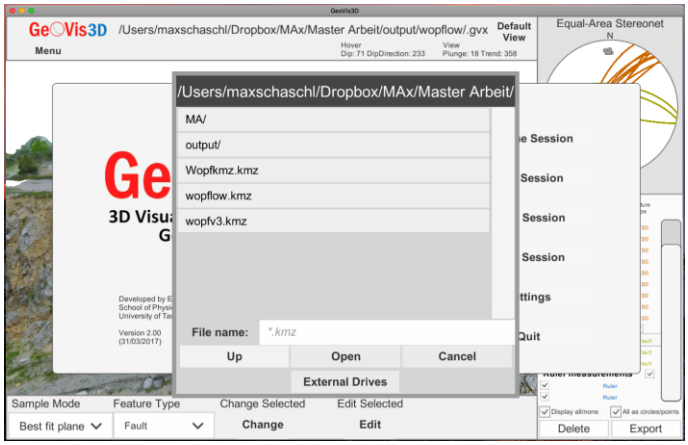

Figure 10: File context menu.

In the middle, the model appears which can be moved and turned using the mouse (Fig. 11). By clicking and moving the cursor the model can be turned. By clicking the mouse wheel and moving the mouse, the model can be shifted. Through rotating the mouse wheel it can be zoomed in and out. The menu can be accessed by pressing the “Escape” button, where the session can be saved and the settings edited. It is recommended to twitch the settings for the “zoom-“ and “mouse-sensitivity” to the users belonging. In the beginning, it will take a little time to get used to the control of the 3D view.

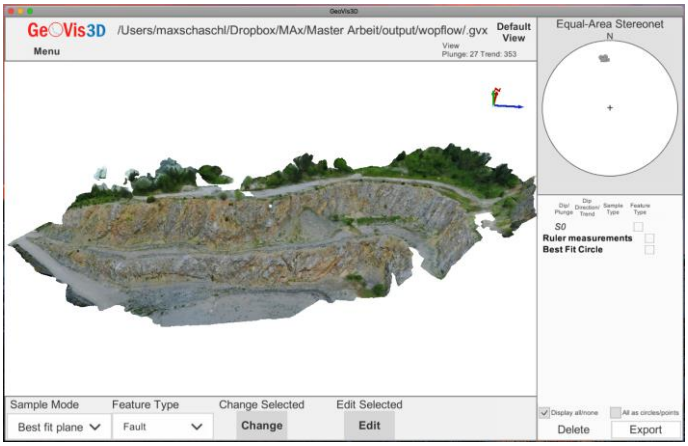

Figure 11: User interface overview with a loaded 3D model.

To start, the “Sample Mode” and “Feature Type” that should get measured have to be chosen (Fig. 12).Then points can be added by double clicking the left mouse button to the surface, which should be measured. At least three points are necessary to create a “Best fit plane”. The plane will be displayed and colored in respect to the quality of the estimation. Green means a good fit, red a bad fit. A plane can be accepted by clicking on “Finish Plane”. The color of a finished plane is only to differ the

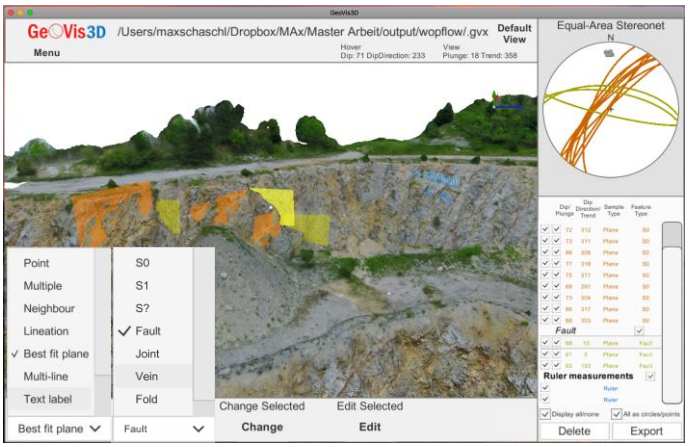

Figure 12: Possible “Sample Modes” and “Feature Types“.

different feature types and is not a quality indicator. The plunge and dip direction will appear in the list and a great circle will be printed in the stereoplot. To measure distances just choose the Sample Mode “Ruler”. Double click to set the first point and second point at the desired positions. A blue ruler with the distance between those two points will emerge.

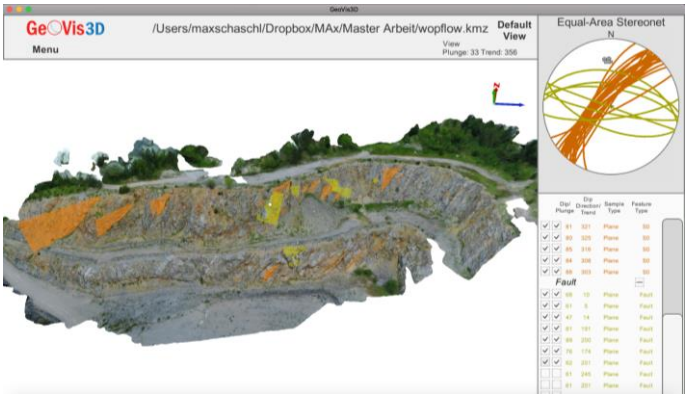

Figure 13: Sampled planes and the corresponding great circles in the stereoplot.

After gathering the desired data the values can be exported into a comma separated values file (.csv), which than can be imported to Excel or other programs capable to read .csv files for further use.

2.3.4.2. CloudCompare

CloudCompare is also an Open Source Project, which was created by Daniel Girardeau-Montaut from Grenobles, France (Girardeau-Montaut, 2015). It is a 3D point cloud and mesh processing software with the main task to compare different point clouds with each other like the detection of a subsidence. Due to the effort of a whole lot of people, over the time different plugins were created with a diverse field of application.
Two of them are of very high interest for geological tasks due to their powerful abilities:

- qFacets
- qCompass

User Interface

CloudCompare can be freely downloaded from http://www.cloudcompare.org.
The Point Cloud has to be exported from AgiSoft PhotoScan by clicking on File → Export Points. It is recommended to export the Cloud as a .ply file because the size is compressed in comparison to a .obj file. This provides a better handling and less computational power. The coordinates parameter has to be set to “Local Coordinates” instead of WGS84 (Default Setting).
By clicking “Open” in CloudCompare a point cloud can be loaded. It will take a few seconds, depending on the size of the model, to be loaded. Now the point cloud can be further processed. With "click and hold" the left mouse button the cloud can be paned in all three axes. With

"click and hold" the right mouse button the cloud can be moved. Depending on the size of the object and the density of the dots, the representation of the surface at a high zoom can be poor. For this, the point size can be varied to get a better illustration. If the cursor is moved to the left corner of the "3D View" window, a display with "default point width" and "default line width" appears. Here the size of the points can be adjusted and, if present, lines (Fig. 14). On the very left side and upper side of the window, the toolbars can be found with various symbols. The left toolbar contains mostly display options like "Front View", "Top View" etc. and on the topside the most important editing tools can be found. Next to the toolbar, two windows are displayed: "DB Tree" which stands for database directory and "Properties". In the "DB Tree", first the loaded point cloud is shown. There, similar to a folder structure, the features generated in the course of editing are displayed and can be managed. If a feature is highlighted by clicking, no matter if in the "DB Tree" or in the 3D view, its properties will be shown in the "Properties" window. At the bottom of the window is the "Console", where error messages and the like are displayed.

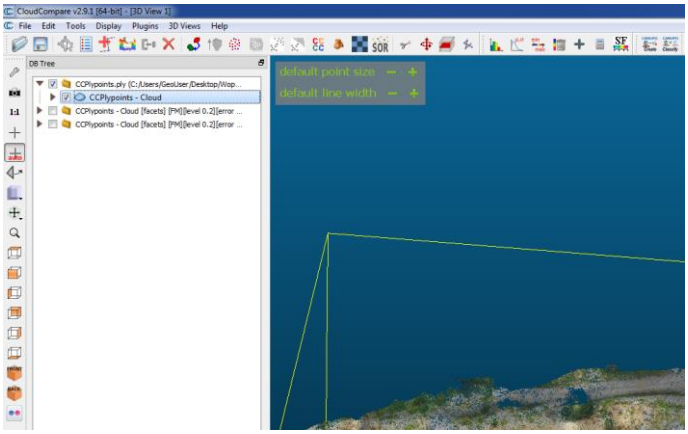

Figure 14: Point- and line size options.

The first step is the calculation of the normals. Therefore select the point cloud, go to "Edit" → "Normals" → "compute" (Fig. 15). Use the default settings, which mostly work properly. Regarding to the size of the point cloud and the power of the PC this step may take a few minutes. Now the cloud is ready for further validation using the different plugins.

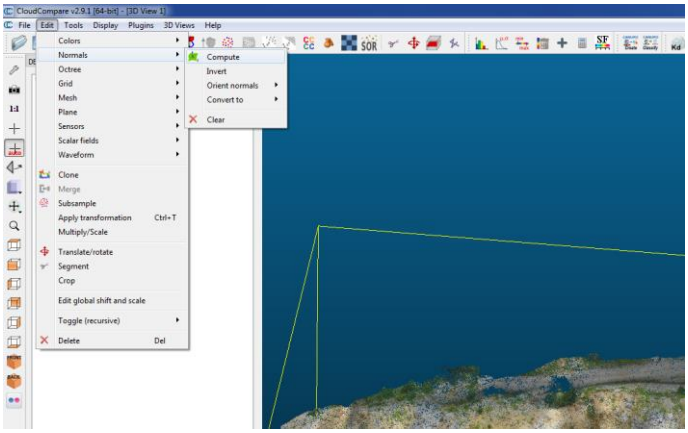

Figure 15: Context menu for the computation of the "Normals".

qFacets

Thomas Dewez, from the BRGM – France Geological Survey (Dewez et al., 2016), created the "qFacets" plugin to extract planar facets of point clouds and calculate their strike and dip values. The achieved data can be grouped and plotted separately in stereograms. The point classification is done by two different algorithms called „Kd-Tree" and „Fast Marching",

whereas the latter turned out to deliver the better results. The output data of the plugin are the interactive stereograms and the possibility to export the facets into shapefiles for further use in GIS software or as comma-separated ASCII file.

Workflow

This plugin will detect every planar surface and their dip / dip direction depending on the settings made. To start the process go to „Plugins“ → „Facet / Fracture detection“ → „Extract Facets (Fast Marching)“ (Fig. 16). There is also the option „Extract Facets (Kd-Tree)“ which has shown not to be as accurate than the „Fast Marching“ algorithm. After clicking „Extract Facets (Fast Marching)“ a pop up with different settings will appear. It is recommended to use the default settings for the first iterations (Fig. 17). The „Min points per facet“ option which indicates the minimum amount of points to create a facet can be used to define the “facet resolution”. The lower the amount the more facets, the higher the resolution. Disadvantage of a to low points per facet count is the higher computational time needed and that „quasi-planar“ surfaces get split into a lot of small facets with only a minimal difference in dip and dip direction. In conclusion it takes a few iterations to get a convenient „facet resolution“ depending on the requirements. The facets are displayed in the “3D View” in different colours reliant on their dip and direction and as folders in the “DB Tree” as shown in Figure 18 and 19.

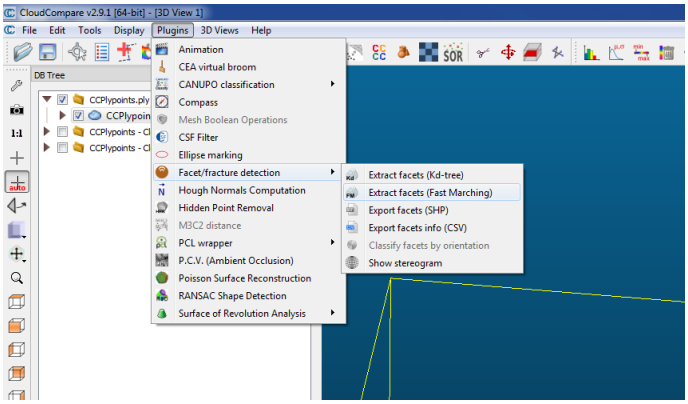

Figure 17: Contextmenu for Facet / Fracture detection.

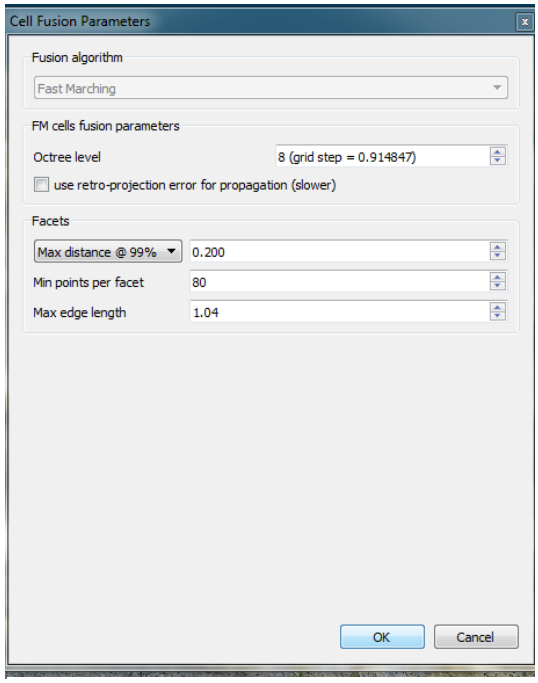

Figure 16: Cell Fusion Parameters. Default settings recommended for the first iterations.

For simplicity, the individual facets can be grouped. To do this, select the main folder of the facets in the "DB Tree", click on "Plugins" → "Facet / Fracture detection" → "Classify Facets by orientation". Now a menu appears where the step size for the classification can be chosen. The result is a folder structure in the "DB Tree", which is numbered consecutively and named

after the class. Now there is the possibility to toggle the visibility of the different classified folders, which manifests in the “3D View” by the disappearance of the facets within the range of the folders bandwidth.

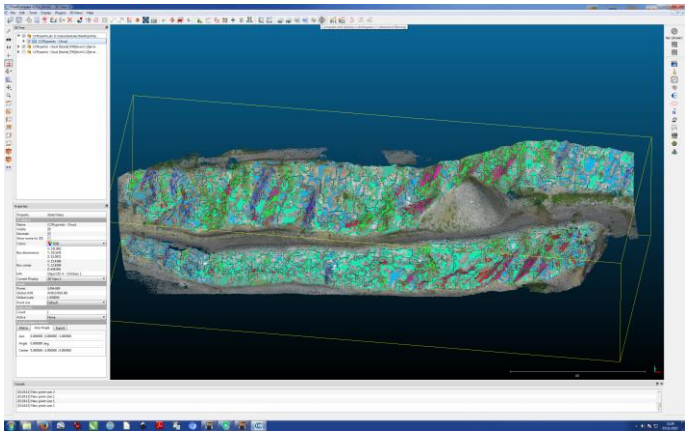

Figure 18: Point Cloud with facet overlay.

Another feature is the interactive Stereogram that makes it possible to plot every facet, and filter the displayed facets in the “3D View”. Proceed to "Plugins" → "Facet / Fracture detection" → “Show Stereogram”. A pop up appears to set the “main sectors step” and the “resolution” where the latter indicates what band-width of dip / dip direction will be summarized in the Stereogram.

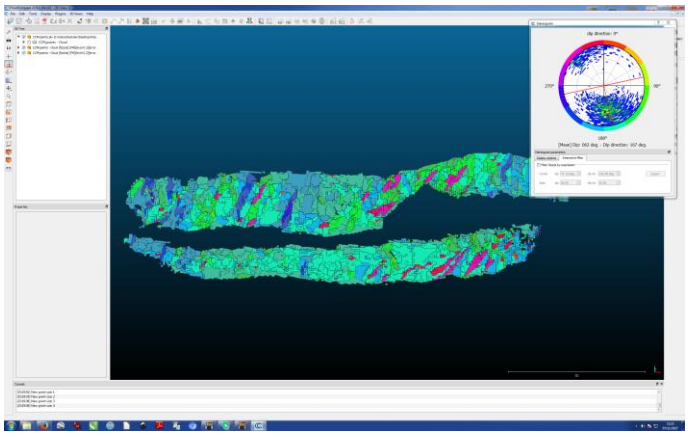

Figure 19: Unnecessary facets have been removed

In the “Stereogram” window, the mean dip and dip direction will be shown underneath the plot. The colours indicate the density of facets in the given sector of the Stereogram. Two tabs are available the first, “Display options” to twitch the formatting, in the second tab the “Interac-tive filter” further filter options are displayed. To apply the filter selections, toggle the tick box “Filter facets by orientation”. A pink sec-tor in the Stereogram will appear that can be moved to the region of interest by clicking on the accordingly area. Only the facets plotting within the range of the pink field will be dis-played in the “3D View” window. The area of the filter can be modified in the four input fields underneath the plot. The filtered facets

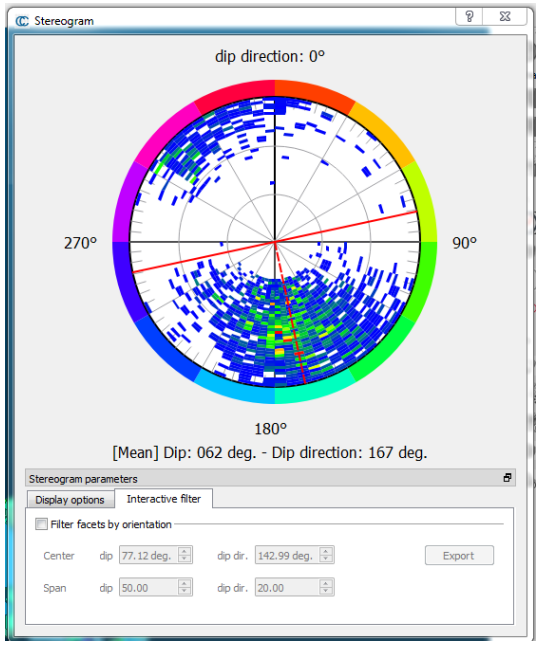

Figure 20: The Stereogram shows the facet distribution and density

can be exported into an own folder directory in the “DB Tree” just by clicking the “Export” button.

The calculated facets also can be exported as shapefiles for the further use in GIS applications. An important point to get a proper result for the investigation of different planes and faults is to eliminate facets that obviously do not belong to the area of interest. This would influence the result due to a distorted distribution of the dip and dip directions.

In summary qFacets provides a suitable quantitative overview in terms of the orientation distribution of outcrops surfaces and presents the data in an easy to interpret manner. The quantitative data is of high interest for geo-engineering applications, where the origin of a planes orientation is of minor importance.

Advantages / Disadvantages

The main focus of this plugin is the quantitative evaluation of surfaces with the advantage of a comprehensive result. The disadvantage of this plugin is the sheer amount of evaluated areas on large models, which makes it difficult to find a middle way between the resolution of the evaluation intervals and the accuracy. Furthermore, the computing power and thus the file size limits the practicability. Due to its quantitative manner, there is a lot of space for the interpretation of the results.

qCompass

This plugin can be described as a virtual mapping geologist and contains two different modes, the „Compass Mode“ and the „Map Mode“. In “Compass Mode”, it is possible to measure planes for their dip and dip direction values but in difference to qFacets the work has to be done by picking points. Another feature is the semi-automatically trace function for features like fractures, joints and veins. All data is stored in a measurements folder (Thiele et al., 2017).

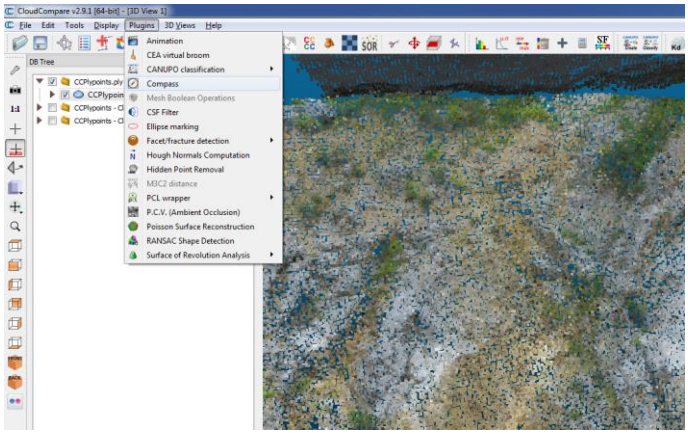

Figure 21: Context menu for the different plugins.

Workflow

qCompass is a lightweight and easy to use plugin. By clicking on „Plugins“ → „Compass“ (Fig. 21) the Compass toolbar will be shown (Fig. 22). The first two icons stand for the “Compass” or “Map Mode”. In the compass mode three relevant tools are available: “Plane Tool”

to measure plane surface orientations, “Trace Tool” to measure orientations from linear features like veins, joints, faults, etc. and the “Lineation Tool” to measure distances and the orientation of lineations. When the “Plane Tool” is active, a red dotted circle appear around the cursor. This circle determines the area of which the plane orientation will be calculated. When zooming in or out the circle diameter remains constant, which means to measure bigger areas the view has to be zoomed out and vice versa. Click on the area of interest, a green best-fit plane will show up with a normal oriented in the corresponding dip and dip direction and a new folder in the “DB Tree” called “measurements” will be created (Fig. 23). This folder will contain all the following measurements done. The “Plane Tool” measurements are always named after their dip / dip direction. In the properties of a measurement, it is possible to toggle the visibility, normal and the name in the “3D View”.

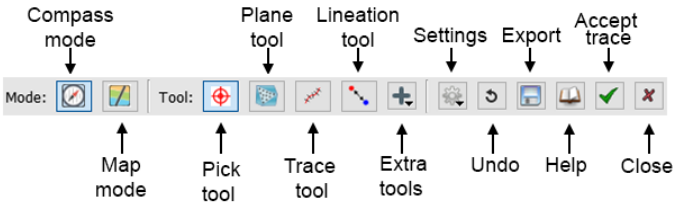

Figure 22: qCompass menu bar.

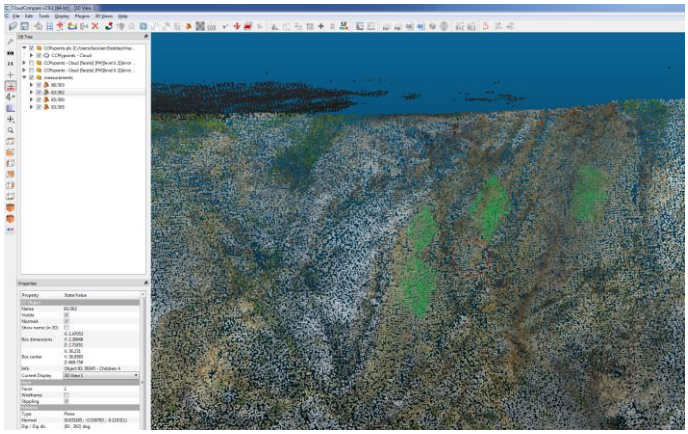

Figure 23: "Plane Tool" measurements.

The second tool is the “Trace Tool” to semi-automatic track linear features. By setting points on the ends of a linear feature a “least coast” trace will be calculated and displayed (Fig. 24). For further information of the algorithm behind the tool, read Thiele et al., (2017). In addition, multiple points can be set to avoid failures for longer features. The trace can be finished by clicking on the green tick in the menu bar.

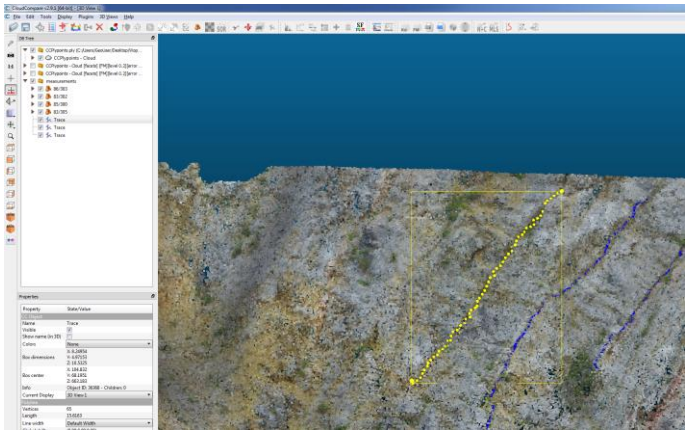

Figure 24: "least coast" traces of linear features.

The “Lineation Tool” is similar in the way to use. A start- and end- point have to be selected to define the lineation. An arrow visualizes the feature in the “3D View” and an object named after the properties will be created in the measurement folder. The first part of the name describes the length, the second part the dip and dip direction.

The “Mapping Mode” offers the same tools like the “Compass Mode” but in addition, so called “GeoObjects” are implemented. Those can be defined by an upper boundary, interior and lower boundary. The “Mapping Mode” can be compared to a digital field book where measurements and in addition comments can be summed up to describe the geology (Fig. 25).

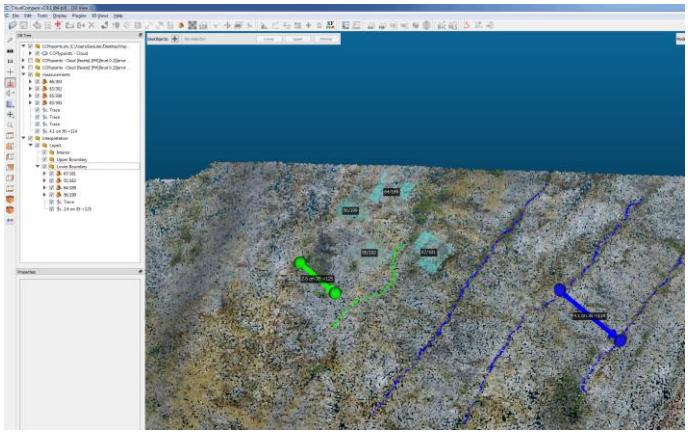

Figure 25: Planes, lineations, and fracture traces

Advantages / Disadvantages

This plugin is better suited for the evaluation of smaller models. In any case, here is the possibility of a qualitative evaluation of individual areas similar to GeoVis3D. Another advantage is the very simple and intuitive application of the plugin. The biggest disadvantage in comparison is the lack of a visualization of the orientation data like the stereoplots implemented in the qFacets plugin and GeoVis 3D.

2.3.4.3. Others

The programs listed above are the most valuable programs for geological purpose but there is still a lot of other software to edit, registrate, filter, etc. point clouds or meshes.

Meshlab, like all the previously mentioned programs, is grown as an open source project, driven by the Visual Computing Lab of the ISTI-CNR in Pisa, Italy (Cignoni et al., 2008). As the name implements this application is specialized on editing 3D meshes, which makes it useful for the generation of 3D printable models. It is equipped with smoothing, cleaning and colorization filters to get the best results out of a raw 3D mesh. One, in a geological meaning, useful tool is the measurement tool. With this, the distance between two points can easily be measured by clicking on them. It is easy to operate in belongs of filtering, smoothing and cleaning algorithms. Additionally, it is very convenient to use because it works with meshes instead of points, which keeps the requirements for the hardware low. The disadvantage is the small affect for geological uses. Only thing what can be done respectively to evaluating purposes is the easy to handle distance measurement tool.

As mentioned in the chapter about AgiSoft before, it is in the meanwhile not only a photogrammetric software. It gained features like the ability to measure distances, areas, volumes and furthermore it is possible to create Digital Elevation Models (DEM).

3DSurvey is a software very similar to AgiSoft Photoscan, with which point clouds can be created with structure from motion methods and some basic measuring tasks like distances, areas, etc. can be done.
A whole branch are the so-called BIM (Building Information Modeling) software solutions like Autodesk Revit or Recap. Those are much more complex, for building and construction purposes specialized tools, which also can use, edit, and work with point clouds derived from photogrammetric applications or laser scanning methods

Depending on the possibilities given by the software and additional plugins the decision for the further data acquisition has been made. GeoVis 3D and CloudCompare with the use of the plugins qFacets and qCompass are the chosen applications. This is due to the fact of what in the means of geological interest these applications are able to investigate.

3. Implementation and Comparison: Quarry Dürnbach

3.1. General

The part of the quarry Dürnbach investigated in this study is currently not active. Topographically the quarry is an open pit with a size of about ~230m from West to East and ~150m from North to South. It consists of three major walls that are separated in two mining terraces that are each approximately 8m in height. The three walls are directed in NNW, NE and SE direction whereas the NNW- and NE wall were examined and reconstructed as 3D model in detail (Figure 26). Daniel Ritzinger investigated the structures in this section of the pit focusing on brittle fault slip data and structures probably associated with larger scale folding and thrust displacement in this area. The results of his field investigations were used for the comparison and evaluation of the photogrammetric derived data.

Figure 26: Overflown area of the Quarry Dürnbach.

The acquisition of the photo set, which contains 684 different pictures, was done in less than 2 hours and was used for the reconstruction of a high-resolution 3D model. The dense point cloud counts 16.000.000 points and the resulting textured mesh consists of 360.000 facets.

3.2. Used Methods and planning

The topography of the pit would in principle allow an automatic grid flight strategy, but because of the changing slope gradients this approach is less efficient than free flight operation. To cover both pit levels, at least two raster flights would have to be performed, each on a different height with individual camera pitch adjustments.

As shown in Figure 26, due to the bottom of the pit, which is very wide in relation to the walls, there would be a lot of unnecessary footage. This would cause the 3D model to be unnecessarily detailed in an area which is of no geological interest. Furthermore, the computation time as well as the requirement for further processing would needlessly increase. The camera positioning in this case is another problem because it is difficult due to the geometry of the pit to ensure a consistently and accurate alignment of the camera in respect to the walls. A problem is the accuracy of the trajectory because it is partly below the pit horizon, which leads to the risk of a collision with the walls.

As presented in Chapter 2.3.1, an automatic terrain-following flight mission using the ground station of UgCS would be possible. Before planning the actual mission, there is the need of the topographical data, which can be gathered either by a foregoing observation flight or by already existing DEM´s. The question arises if the effort, which must be carried out in advance, is in relation to the requested results. Since the University of Vienna is not (yet) in possession of a license for the aforementioned software, only the first two options remain.

Finally, due to the declared preconditions, risks and flight experience, a manual aerial survey was carried out. The drone was largely controlled in the so-called "tripod mode" (for details see Appendix "Brief introduction DJI Mavic"). The camera was operated in automatic mode and triggered manually. The photoset consists of 684 individual pictures, which mostly captured the walls of the pit, which expose the geological structures of interest. A few pictures were taken from a higher altitude to cover the pit floor and prevent holes in the model. The covered length is about 220 m, which was flown on 4-5 different heights. The image distance varies between 3m for undercut areas and about 7-8 m for clearly exposed surfaces. The camera was manually tilted and steadily adjusted to the topography to ensure a perpendicular alignment of the camera to the wall surface. In total, three battery charges with each about 22min flight time were necessary to cover the investigated outcrop in the required detail.

Referring to Equation (1) the GSD is calculated with the following values:

Wsen [mm]	6,2	**Wsen [mm]**	6,2
f [mm]	4,91	**f [mm]**	4,91
AGL [m]	8	**AGL [m]**	3
Wimg [pixel]	4000	**Wimg [pixel]**	4000
GSD [mm/pixel]	**2,53**	**GSD [mm/pixel]**	**0,95**

Table 7: GSD calculation table.

Due to the topography and manual control of the drone the GSD varies between 0,95 mm/Pixel and 2,53 mm/Pixel.

The next step was to generate the 3D model using AgiSoft PhotoScan on the workstation in the Department of Geodynamics and Sedimentology. The PC is equipped with the following components:

Operating System	Microsoft Windows 7 Professional
CPU	Intel® Core™ i7-6700K @ 4x4.00GHz
RAM	32GB
GPU	NVIDIA GeForce GTX 750 Ti 2GB

Table 8: Workstation components.

Unfortunately, the large number of pictures did not allow with the available hardware to calculate the model in the highest possible resolution. The following settings were selected for the various calculation steps in AgiSoft PhotoScan:

General		**Dense Point Cloud**	
Cameras	684	Points	16,231,278
Aligned cameras	684	Quality	Low
Coordinate system	WGS 84 (EPSG::4326)	Depth filtering	Aggressive
Rotation angles	Yaw, Pitch, Roll	Surface type	Arbitrary
PointCloud		Source data	Dense
Points	606,611 of 687,891	Interpolation	Enabled
Alignment parameters		Quality	Low
Accuracy	High	Depth filtering	Aggressive
Generic preselection	Yes	Face count	360,694
Reference preselection	Yes	**Texturing parameters**	
Key point limit	40000	Mapping mode	Generic
Tie point limit	4000	Blending mode	Mosaic
Adap. camera model fitting	Yes	Texture size	8,192 X 8,192
Optimization parameters		Enable colour correction	No
Parameters	f, ex, cy, kl-k3, pl, p2	Enable hole filling	Yes
Fit rolling shutter	No		
Depth Maps			
Count	684		
Quality	Low		
Filtering mode	Aggressive		

Table 9: AgiSoft Photoscan settings and parameters.

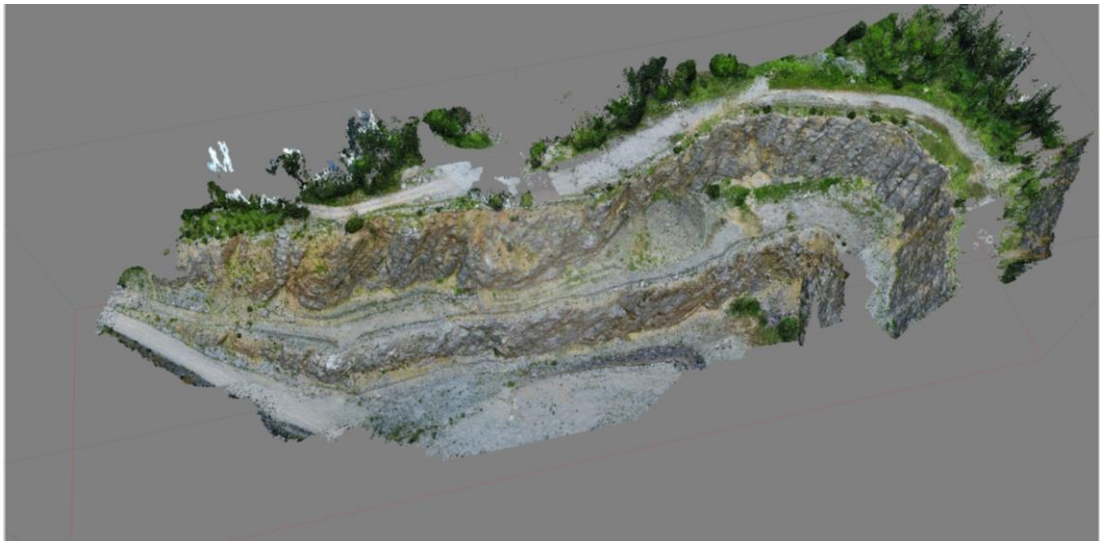

Figure 28: Textured 3D model in Photoscan.

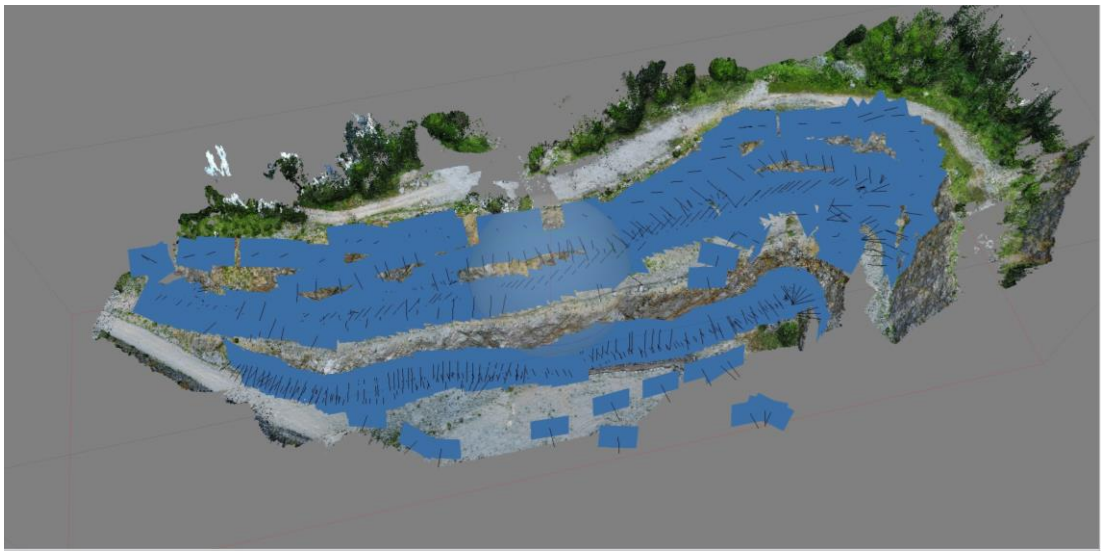

Figure 27: Camera positions of the individual photos.

The created 3D model consists of 16.231.278 points and 360.694 facets (Table 9), which was then exported into the different required output formats for the analysis.

4. Results and discussion

4.1. Results GeoVis 3D

For post-processing and data evaluation GeoVis3D and CloudCompare were used. In GeoVis 3D, obvious bedding surfaces as well as faults were manually traced and automatically measured. In CloudCompare, the complete outcrop was measured using the qFacets plugin. In Ge-

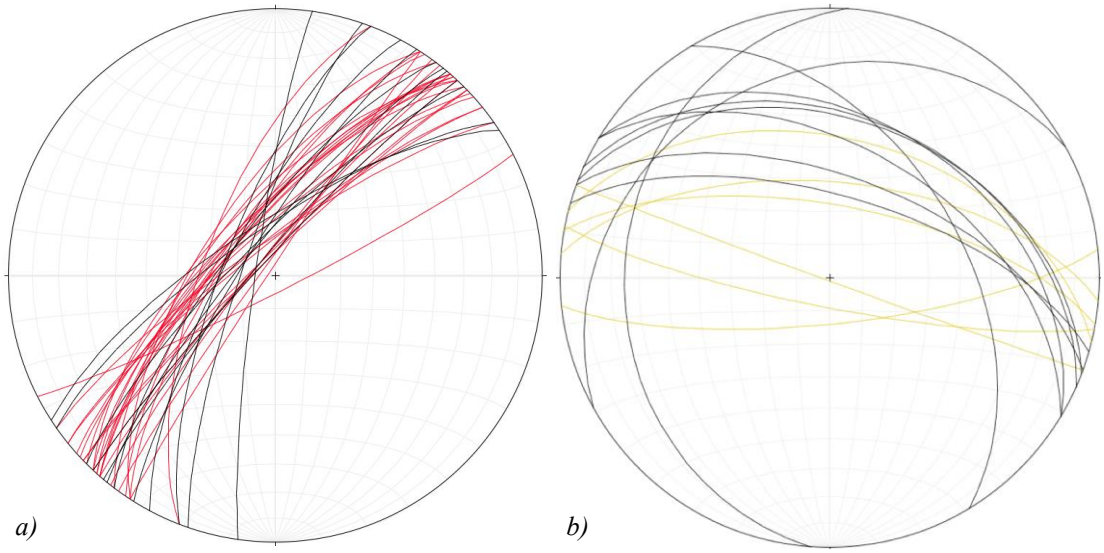

a) b)

Figure 29: a) In red the great circle plots of the bedding plane orientation. b) In yellow the great circles of the fault orientations.

oVis 3D, 26 different bedding planes and 6 fault planes have been distinguished. The bedding planes show a steep dip between 69° to 88° with an azimuth direction of 291° to 325° (WNW – NW) as shown in Figure 29 a). The average bedding surface orientation values 305,2° azimuth and a dip of 77,3° (Table 10). The faults cut the bedding planes mostly in N direction and dipping with intermediate angles of around 60°-80° (Fig. 29 b).

4.2. Results CloudCompare

The great number of points in the cloud made it almost impossible to work with CloudCompare. Therefore, a second Dense Point Cloud was created with the lowest settings and cropped as much as possible. In addition, the northeastern part was removed because the wall turns 90 ° and thus would distort the results examined with the qFacets plugin. Due to the scale of the model, only bedding surfaces and large faults can be distinguished from one another. The

output stereogram created by the plugin (Fig. 30) shows two areas with a high density of orientations.

Also manual measurements with the qCompass "Plane Tool" have been performed.

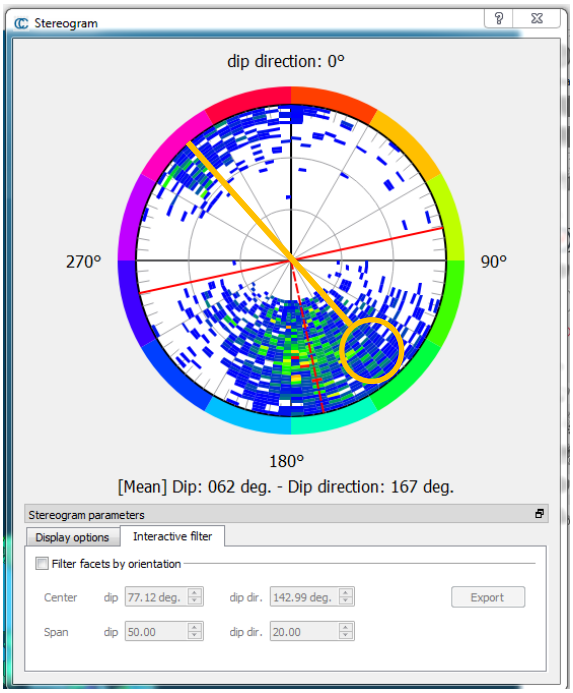

Figure 30: qFacets Stereogram. Two major dense areas can be distinguished. The orange line and circle determines the overtilted planes.

4.3. Discussion

The first patch in the NW quadrant represents the bedding planes, which correlates very good with the data extracted from GeoVis 3D. Those facets are represented in pink and red. A second patch is located in the S – SE area. A not to be despised portion of the facets in this sector exhibit partly by 180° the dip directions of the bedding planes (Fig. 30 orange circle). This is due to the "facet – resolution" and the partial

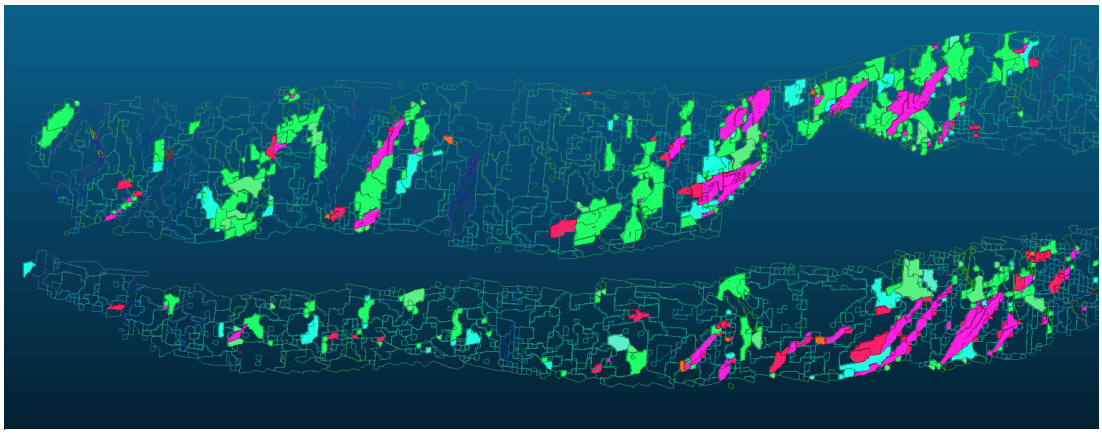

Figure 31:"Splitted" faces due to the facet resolution parameters. Pink and green colours illustrate the orientation.

over-tilting of the bedding planes. A surface which in GeoVis 3D was measured as one big plane is in the qFacet evaluation, split into a few different facets as seen in Figure 31. This argument could be examined and confirmed using the "Plane Tool" provided with the qCompass plugin (Fig. 32). The other part of this dense section might refer to the slope area due to

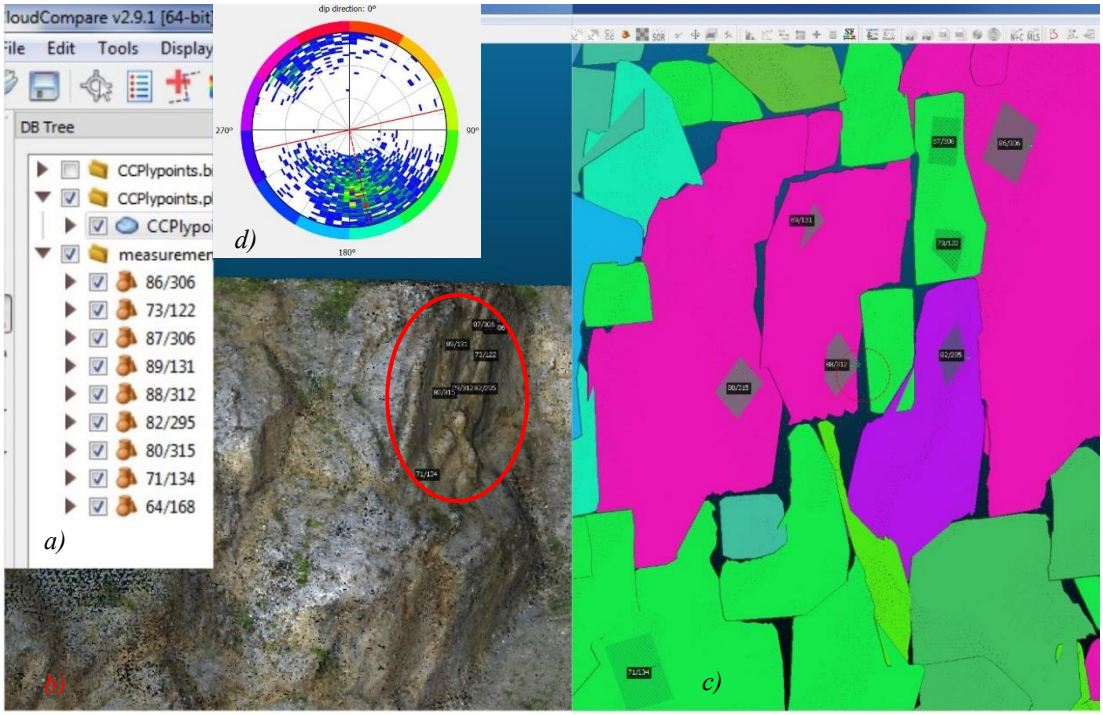

Figure 32:This figure shows the reason of some facets dip orientation rotated by 180°. a) The measurements carried out with the "Plane Tool". b) Shows the overview of the investigated area. c) The facets extracted with the qFacets plugin can be seen. By comparing with the colour-coded stereogram d), the facets and the investigated area in b) the problem can be distinguished.

the old mining operations. In comparison with the field compass measurements of Daniel Ritzinger, a high agreement can be found. The Figure 29 a) shows the manual measured bedding planes in black and the digitally distinguished ones in red. The average values for the bedding planes measured by Daniel Ritzinger and digitally evaluated are as follows:

Method	Dip Direction	Dip
Manual	305,5°	78,8°
GeoVis 3D	305,2°	77,3°
Δ	0,3°	1,5°

Table 10: Comparison of the average bedding plane orientations.

The dataset comprises 12 samples of manual measurements and 26 digital measurements. As shown in Table 10 the deviation of the dip direction averages only 0,3° and of the dip 1,5°. The comparison of the faults in Figure 29 b) show a good consensus and a few discordant values. This might be due to the different scales the measurements were performed. Small faults and fault surfaces could only be recognized classical fieldwork due to the resolution of the 3D model. The results speak for themselves and can certainly be considered as very good and reliable. Compared to the manual measurements, the deviations are so small that they are unlikely to be noticed in the interpretation of the geological conditions. Even though the fact that no geo-referencing using GPS reference points was performed. Only the GPS metadata of the photos was available.

5. Conclusion and outlook

Although the potential of 3D photogrammetry and its products is known, it is far from exhausted. The opportunities that come with it are very promising, but much work still needs to be invested in the development of comprehensive evaluation programs. However, the basic building blocks are already laid with the programs described in this work. A few opportunities are available at the moment, but unfortunately over detours or not very intuitive to use.
Suggestions for improvement and findings:

- Depending on the size of the point clouds, the handling is limited during further post processing. There is a trade of between lower accuracy and efficient handling on standard PC.
- Currently, there is no adequate "all in one" software solution to meet all needs for geological data collection from photogrammetry models. Various programs offers different solutions for structural measurements from photogrammetric models.
- The training in the various software applications is time consuming. Although various tutorials exist for different software solutions a worked through geological examples and description of the necessary software tools is still missing.
- Hardly any program allows interactive editing, as it is widely known form CAD programs. For example, inserting specific faces or filling individual holes in a model is not straight forward and requires very good knowledge of workarounds in the programs.
- A trade-off between details preserved in the models and clumsy handling of huge data has to be individually determined. Excessive amounts of data can lead to severe problems with computer memory and speed of calculations.
  The major advantage of the presented methods are:
  By archiving the 3D model, new measurements can be applied at any time and new methods of analysis can be used without the hassle of revisiting the area.
  Digital archiving of outcrops can be used to carry out long-term studies on erosion, rock mass movement and subsidence.
  Similar projects like the AUSGEOL project of Dr. Michael Roach can be carried out all over the world to preserve important information for the future and make it accessible for the community.

In some of these cases, much work will be needed in the future to better cover the requirements for geologically relevant purposes. It would be desirable to have a software package that allows comprehensive editing. Exempels are:

- The easy closing of holes.
- Inserting surfaces.
- Simple methods for creating a closed 3D vowel body from the actual 2.5D surface in the sense of creating 3D printing.
- Editing as a mesh and not point clouds, as they require much less computational effort.
- Visualization of measured features like implemented in GeoVis 3D (Stereoplot).
- Colour-based bedding and foliation extracting algorithms

New remote sensing techniques can greatly simplify mapping and advance digitization. Such “digital outcrops” provide faster and more accurate results, but also affects economic aspects such as time and cost savings in planning, monitoring and documentation of projects. Due to mass movements (Jaboyedoff et al., 2012) and rock-slope processes (Abellán et al., 2014), it is possible that impoundments of streams and rivers occur, which subsequently expose the adjacent areas to flooding (Reitner et al., 2011). In such cases, the rapid 3D model conception by the use of drones leads to fast preventative measures and risk assessments for the affected areas. This can protect land and life, especially in impassable and underdeveloped areas.

In conclusion, digital outcrop geology is a research field “in progress” with an enormous potential for the future. Increase in hardware power and performance will open a new dimension for the interactive construction of high-resolution outcrop models.

References

Abellán, A., Oppikofer, T., Jaboyedoff, M., Rosser, N. J., Lim, M., & Lato, M. J. (2014). Terrestrial laser scanning of rock slope instabilities. *Earth surface processes and landforms*, *39*(1), 80-97.

AgiSoft, L. L. C., St Petersburg, R. (2017). Agisoft photoscan. *Professional Edition*. Manual retrieved September 20, 2017 from http://www.agisoft.com/pdf/photoscan-pro_1_3_en.pdf

Bemis, S. P., Micklethwaite, S., Turner, D., James, M. R., Akciz, S., Thiele, S. T., & Bangash, H. A. (2014). Ground-based and UAV-based photogrammetry: A multi-scale, high-resolution mapping tool for structural geology and paleoseismology. *Journal of Structural Geology*, *69*, 163-178.

Blistan, P., Kovanič, Ľ., Zelizňaková, V., & Palková, J. (2016). Using UAV photogrammetry to document rock outcrops. *Acta Montanistica Slovaca*, *21*(2).

Carrivick, J. L., Smith, M. W., & Quincey, D. J. (2016). *Structure from Motion in the Geosciences*. John Wiley & Sons.

Cignoni, P., Callieri, M., Corsini, M., Dellepiane, M., Ganovelli, F., & Ranzuglia, G. (2008). Meshlab: an open-source mesh processing tool. *Eurographics Italian Chapter Conference Vol. 2008,* 129-136.

Decker, K., Peresson, H., & Faupl, P. (1994). Die miozäne Tektonik der östlichen Kalkalpen: Kinematik, Paläospannungen und Deformationsaufteilung während der "lateralen Extrusion" der Zentralalpen. *Jahrbuch Geol Bundesanstalt*, *137*, 5-18.

Dewez, T. J., Girardeau-Montaut, D., Allanic, C., & Rohmer, J. (2016). Facets: A CloudCompare plugin to extract geological planes from unstructured 3D point clouds. *International Archives of the Photogrammetry, Remote Sensing & Spatial Information Sciences*, *41*.

GeoVis3D - freeware for analysis and annotation of virtual 3D geological models. Retrieved July 16, 2017 from http://www.ausgeol.org/geovis3d/

Girardeau-Montaut, D. (2015). Cloud Compare 3D Point Cloud and Mesh Processing Software. *Open Source Project*.

Jaboyedoff, M., Oppikofer, T., Abellán, A., Derron, M. H., Loye, A., Metzger, R., & Pedrazzini, A. (2012). Use of LIDAR in landslide investigations: a review. *Natural hazards*, *61*(1), 5-28.

Linder, W. (2009). *Digital photogrammetry*. Springer.

Mandl, G. W. (2000). The Alpine sector of the Tethyan shelf—examples of Triassic to Jurassic sedimentation and deformation from the Northern Calcareous Alps. *Mitteilungen der Österreichischen Geologischen Gesellschaft,* 92(1999), 61-77.

Nex, F., & Remondino, F. (2014). UAV for 3D mapping applications: a review. *Applied Geomatics*, *6*(1), 1-15.

Piller, W. E., Egger, H., Erhart, C. W., Gross, M., Harzhauser, M., Hubmann, B., ... & Lukeneder, A. (2004). Stratigraphische Tabelle von Österreich 2004 (sedimentäre Schichtfolgen). *Österreichische Stratigraphische Kommission.*

Pix4D. Pix4Dcapture App. Retrieved July 14, 2017 from https://pix4d.com/product/pix4dcapture/

Reitner, J. & Linner, M. (2011). Lienz and surrounding. *2nd Conference on Slope Tectonics 6 - 11 September 2011 Vienna, Austria: Field Trip Guide on Austrian Deep-Seated Slope Failures*. 41-55

Schenk, T. (2005). Introduction to Photogrammetry. Retrieved September 20, 2017 from http://www.mat.uc.pt/~gil/downloads/IntroPhoto.pdf

Schober, A., Delleske, R., Hartmeyer, I., Keuschnig, M. (2017). Using Unmanned Aerial Systems (UAS) for the monitoring of protective constructions in steep, inaccessible terrain, Pass Lueg, Austria. *6th Interdisciplinary Workshop on Rockfall Protection RocExs 2017, Barcelona, Spain,* 205-208.

Summesberger, H. (1991). Geologische Karte der Republik Österreich 1: 50.000, Blatt 75, Puchberg am Schneeberg. Wien (Geol. B-. A.).

Thiele, S. T., Grose, L., Samsu, A., Micklethwaite, S., Vollgger, S. A., & Cruden, A. R. (2017). Rapid, semi-automatic fracture and contact mapping for point clouds, images and geophysical data. Solid Earth Discuss., https://doi.org/10.5194/se-2017-83, in review.

Tollmann, A. (1976). *Der Bau der nördlichen Kalkalpen: orogene Stellung u. regionale Tektonik* (Vol. 3). Deuticke.

Tonkin, T. N., & Midgley, N. G. (2016). Ground-control networks for image based surface reconstruction: an investigation of optimum survey designs using UAV derived imagery and structure-from-motion photogrammetry. *Remote Sensing*, *8*(9), 786.

Vollgger, S. A., & Cruden, A. R. (2016). Mapping folds and fractures in basement and cover rocks using UAV photogrammetry, Cape Liptrap and Cape Paterson, Victoria, Australia. *Journal of Structural Geology*, *85*, 168-187.

Wessely, G. (2006). *Niederösterreich: Geologie der österreichischen Bundesländer*. Geologische Bundestanstalt.

Wopfinger Rohstoffe. Retrieved August 8, 2017 from http://www.wopfingerbaustoffe.at/front_content.php?idcat=547